



HAL
open science

Enhanced clinical phenotyping by mechanistic bioprofiling in heart failure with preserved ejection fraction: insights from the MEDIA-DHF study (The Metabolic Road to Diastolic Heart Failure)

Susan Stienen, Joao Pedro Ferreira, Masatake Kobayashi, Gregoire Preud'Homme, Daniela Dobre, Jean-Loup Machu, Kévin Duarte, Emmanuel Bresso, Marie-Dominique Devignes, Natalia López Andrés, et al.

► **To cite this version:**

Susan Stienen, Joao Pedro Ferreira, Masatake Kobayashi, Gregoire Preud'Homme, Daniela Dobre, et al.. Enhanced clinical phenotyping by mechanistic bioprofiling in heart failure with preserved ejection fraction: insights from the MEDIA-DHF study (The Metabolic Road to Diastolic Heart Failure). *Biomarkers*, 2020, 25 (2), pp.201-211. 10.1080/1354750X.2020.1727015 . hal-02732968

HAL Id: hal-02732968

<https://hal.univ-lorraine.fr/hal-02732968v1>

Submitted on 2 Jun 2020

HAL is a multi-disciplinary open access archive for the deposit and dissemination of scientific research documents, whether they are published or not. The documents may come from teaching and research institutions in France or abroad, or from public or private research centers.

L'archive ouverte pluridisciplinaire **HAL**, est destinée au dépôt et à la diffusion de documents scientifiques de niveau recherche, publiés ou non, émanant des établissements d'enseignement et de recherche français ou étrangers, des laboratoires publics ou privés.

Enhanced Clinical Phenotyping by Mechanistic Bioprofiling in Heart Failure with Preserved Ejection Fraction: Insights from the MEDIA-DHF study (The Metabolic Road to Diastolic Heart Failure)

Susan Stienen, MD, PhD¹; João Pedro Ferreira, MD, PhD^{1,2}; Masatake Kobayashi, MD¹; Gregoire Preud'homme MSc¹; Daniela Dobre^{1,3}, Jean-Loup Machu, MSc¹; Kevin Duarte PhD¹; Emmanuel Bresso, PhD⁴; Marie-Dominique Devignes, PhD⁴; Natalia López Andrés, PhD⁵; Nicolas Girerd, MD, PhD¹; Svend Aakhus^{6,7}; Giuseppe Ambrosio⁸; Hans-Peter Brunner-La Rocca, MD, PhD⁹; Ricardo Fontes-Carvalho¹⁰; Alan G. Fraser¹¹; Loek van Heerebeek, MD, PhD¹²; Stephane Heymans^{13,14,15} Gilles de Keulenaer¹⁶; Paolo Marino¹⁷; Kenneth McDonald¹⁸; Alexandre Mebazaa¹⁹; Zoltán Papp, PhD²⁰; Riccardo Raddino²¹; Carsten Tschöpe²²; Walter J. Paulus, MD, PhD²³; Faiez Zannad, MD, PhD¹ ¥; Patrick Rossignol, MD, PhD¹ ¥

¹ Université de Lorraine, INSERM, Centre d'Investigation Clinique et Plurithématique 1433, INSERM U1116, CHRU de Nancy, F-CRIN INI-CRCT (Cardiovascular and Renal Clinical Trialists), Nancy, France;

² Department of Physiology and Cardiothoracic Surgery, Cardiovascular Research and Development Unit, Faculty of Medicine, University of Porto, Porto, Portugal;

³ Clinical research and Investigation Unit, Psychotherapeutic Center of Nancy, Laxou, France

⁴ LORIA (CNRS, Inria NGE, Université de Lorraine), Campus Scientifique, F-54506, Vandœuvre-lès-Nancy, France;

⁵ Navarrabiomed, Complejo Hospitalario de Navarra (CHN), Universidad Pública de Navarra (UPNA), IdiSNA. Pamplona. Spain ;

⁶ Oslo University Hospital, Oslo, Norway

⁷ ISB, Norwegian University of Science and Technology, Trondheim, Norway;

⁸ Division of Cardiology, University of Perugia School of Medicine, Perugia, Italy;

⁹ Department of Cardiology, Maastricht University Medical Center, Maastricht, the Netherlands;

¹⁰ Department of Surgery and Physiology, Cardiovascular Research Unit (UnIC), Faculty of Medicine, University of Porto, Porto, Portugal;

¹¹ Wales Heart Research Institute, Cardiff University, Cardiff, United Kingdom;

¹² Department of Cardiology, Onze Lieve Vrouwe Gasthuis, Amsterdam, the Netherlands;

¹³ Department of Cardiology, CARIM School for Cardiovascular Diseases Faculty of Health, Medicine and Life Sciences, Maastricht University, The Netherlands.

¹⁴ Department of Cardiovascular Sciences, Centre for Molecular and Vascular Biology, KU Leuven, Belgium.

¹⁵ William Harvey Research Institute, Barts Heart Centre, Queen Mary University of London, Charterhouse Square, London EC1M 6BQ.

¹⁶ Laboratory of Physiopharmacology, Antwerp University, and ZNA Hartcentrum, Antwerp, Belgium;

¹⁷ Clinical Cardiology, Università del Piemonte Orientale, Department of Translational Medicine, Azienda Ospedaliera Universitaria "Maggiore della Carità", Novara, Italy;

¹⁸ St Michael's Hospital Dun Laoghaire Co. Dublin, Dublin, Ireland;

¹⁹ Department of Anaesthesiology and Critical Care Medicine, Saint Louis and Lariboisière University Hospitals and INSERM UMR-S 942, Paris, France;

²⁰ Division of Clinical Physiology, Department of Cardiology, Faculty of Medicine, University of Debrecen, Debrecen, Hungary ;

²¹ Department of Cardiology, Spedali Civili di Brescia, Brescia, Italy;

²² Department of Cardiology, Campus Virchow-Klinikum, Charite Universitaetsmedizin Berlin, Berlin Institute of Health – Center for Regenerative Therapies (BIH-BCRT), and the German Center for Cardiovascular Research (DZHK ; Berlin partner site), Berlin, Germany;

²³ Amsterdam Cardiovascular Sciences, Amsterdam University Medical Centers, Amsterdam, the Netherlands

¥ both authors contributed equally as last author

Address for correspondence:

Susan Stienen

Centre d'Investigations Cliniques-INSERM CHU de Nancy,

Institut Lorrain du Cœur et des Vaisseaux Louis Mathieu,

4 Rue du Morvan, 54500 Vandoeuvre lès Nancy, France.

E-mail: s.stienen@amc.uva.nl

Abstract

Background

Heart failure with preserved ejection fraction (HFpEF) is a heterogeneous syndrome for which clear evidence of effective therapies is lacking. Understanding which factors determine this heterogeneity may be helped by better phenotyping. An unsupervised statistical approach applied to a large set of biomarkers may identify distinct HFpEF phenotypes.

Methods

Relevant proteomic biomarkers were analyzed in 392 HFpEF patients included in Metabolic Road to Diastolic HF(MEDIA-DHF). We performed an unsupervised cluster analysis to define distinct phenotypes. Cluster characteristics were explored with logistic regression. The association between clusters and 1-year cardiovascular (CV) death and/or CV hospitalization was studied using Cox regression.

Results

Based on 415 biomarkers we identified 2 distinct clusters. Clinical variables associated with cluster 2 were diabetes, impaired renal function, loop diuretics and/or betablockers. Additionally, 17 biomarkers were higher expressed in cluster 2 vs. 1. Patients in cluster 2 vs. those in 1 experienced higher rates of CV death/CV hospitalization (adj.HR 1.93,95%CI 1.12-3.32,p=0.017). Complex-network analyses linked these biomarkers to immune system activation, signal transduction cascades, cell interactions, and metabolism.

Conclusion

Unsupervised machine-learning algorithms applied to a wide range of biomarkers identified 2 HFpEF clusters with different CV phenotypes and outcomes. The identified pathways may provide a basis for future research.

Keywords:

HFPEF, machine learning, biomarkers, cluster analysis, phenotype, complex-network analysis

Introduction

Heart failure with preserved ejection fraction (HFpEF) is a clinical syndrome with multiple causes, and little evidence for effective therapies (Ponikowski et al., 2016). The increasing prevalence of HFpEF and its poor prognosis both make it important to understand the factors contributing to the heterogeneity of the syndrome and its underlying mechanisms (Tsao et al., 2018).

Several studies have sought to identify distinct HFpEF phenotypes based on clinical, echocardiographic and hemodynamic characteristics (Kao et al., 2015; Sanchez-Martinez et al., 2018; Shah et al., 2015; Tabassian et al., 2018). Additionally, biomarkers have also been studied in an attempt to identify HFpEF subgroups with different characteristics and prognosis (Hage et al., 2017; Sanders-van Wijk et al., 2015; Santhanakrishnan et al., 2012; Tromp et al., 2017; Tromp et al., 2018). In these studies, only a limited number of biomarkers were assessed (up to a maximum of 92 biomarkers). Whether a wider biomarker panel may provide further information on the pathophysiology of HFpEF is yet to be determined.

In this study, we performed unsupervised machine-learning algorithms using 415 proteomic biomarkers to identify HFpEF potential mechanistic phenotypes in a prospective observational cohort of HFpEF patients (The Metabolic Road to Diastolic Heart Failure study (MEDIA-DHF); NCT02446327).

Methods

Study population

Between 2012 and 2014, 626 patients were enrolled in MEDIA-DHF ((NCT02446327) which was a multicenter, multinational, observational study in 10 centers (listed in *Supplemental table 1*). After standardized echocardiography (*Supplemental data*) and/or local natriuretic peptide measurements, eligible patients were included when they had a diagnosis of left ventricular diastolic dysfunction following 2007 ESC consensus recommendations (Paulus et al., 2007). Patients included in MEDIA-DHF presented as: 1) acute decompensated HF patients, or 2) patients recently discharged after admission for an acute HF episode (<60 days), or 3) ambulatory chronic disease patients. At inclusion in the study, data on demographics, clinical parameters, laboratory values (including biomarker measurements), electrocardiography and echocardiography were obtained. Follow-up took place at 3, 6 and 12 months after inclusion in the study.

For this substudy, only patients with available biomarkers were included (N=392; see also the flowchart in *Supplemental figure 1*). There were no biomarker measurements in acute decompensated HF patients. The study protocol complied with the Declaration of Helsinki and was approved by the respective Ethics Committees of the participating institutions. All patients provided written informed consent. (ClinicalTrials.gov Identifier: NCT02446327)

Biomarker measurements

Plasma samples taken at inclusion in the study were analyzed for protein biomarkers (including natriuretic peptides) using 5 different Olink Proseek Multiplex panels: cardiovascular disease (CVD) II, CVD III, Inflammation, Cardiometabolic and Organ damage (Olink Proteomics, Uppsala, Sweden). The characteristics of the biomarkers within the different Olink panels are described in *Supplemental table 2* (and www.olink.com). For this

assay, a proximity extension assay (PEA) technology is used where 92 oligonucleotide-labelled antibody probe pairs per panel may bind to their respective targets in 1 μ L plasma sample (Lundberg, Eriksson, Tran, Assarsson, & Fredriksson, 2011). When bound, they give rise to new DNA amplicons with each ID barcoding their respective antigens. Quantification of the amplicons is subsequently performed using a Fluidigm BioMark HD real-time PCR platform. The PCR platform provides log₂-normalized protein expression (NPX) data and an increase of 1 NPX means a doubling in concentration of the specific biomarker. Forty-five proteins that were below the lower limit of detection (LOD) in more than 50% of the patients, were excluded from further analyses (N=45 biomarkers excluded). For the proteins below the LOD in less than 50% of patients, the LOD value was imputed. A total of 415 protein biomarkers were studied.

Cluster analysis

Pearson correlations were assessed between 415 biomarkers. When two biomarkers were highly correlated (>0.8), the biomarker with the largest mean absolute correlation was excluded. Hence, 66 biomarkers were excluded from further analyses. The optimal number of clusters was determined using the *NbClust* package in R (distance=euclidean, min.nc=2, max.nc=15, method=kmeans, index=alllong). Next, k-means cluster analysis (nstart=1000) was performed with data of 349 biomarkers to partition the patients into separate clusters. There were no missing values for these biomarkers. Cluster stability was verified using *Clusterboot* (B=100, clustermethod=kmeansCBI). Jaccard similarities values were highly stable (cluster 1=0.91; cluster 2=0.93). The cluster analysis resulted in two different patient clusters (clusters 1 and 2).

Network analyses

The FHF-GKB (Fight Heart Failure - Graph Knowledge Box) resource, representing most available public knowledge about human protein-disease, protein-protein and protein-pathway relationships is a customized upgraded version of the EdgeBox provided by the EdgeLeap company (available from: <https://www.edgeleap.com/edgebox/>). FHF-GKB data is extracted from public data sources resulting in 20,386 protein nodes imported from Uniprot("UniProt: the universal protein knowledgebase," 2017), including all biomarkers involved in this study, 28,176 disease nodes from Disease Ontology(Kibbe et al., 2015) and DisGenet(Pinero et al., 2017) and 2,222 pathway nodes from Reactome (v65)(Fabregat et al., 2018). Protein - protein relationships were retrieved from STRING (v10.5) (Szklarczyk et al., 2015), Reactome or WikiPathways(Slenter et al., 2018), Mentha(Calderone, Castagnoli, & Cesareni, 2013), or BioGrid(Chatr-Aryamontri et al., 2017) and protein – pathway relationships from Reactome.

Cardiovascular outcome

The pre-specified endpoint of MEDIA-DHF was a composite of CV death and/or CV hospitalizations (NCT02446327). Clinical outcomes were ascertained by telephone interview and recorded in the electronic case report form (including date and place). For hospitalizations, the letter of discharge was provided, while the death certificate was provided in instances of mortality. The primary outcome of this specific substudy was cardiovascular hospitalizations or cardiovascular death at 12 months. Endpoints were adjudicated by a committee blinded to the biomarker data.

Statistical analyses

Baseline clinical, demographic and echocardiographic characteristics across clusters were compared using chi-square, t-test or Mann-Whitney tests, as appropriate.

To identify clinical variables associated with cluster membership defined by the protein biomarkers, a logistic regression analysis was performed. All variables considered are listed in *Supplemental table 3*. Missing predictor values with <20% of missing values were imputed using linear regression analysis (see *Table 1* for the percentage of missing data for each variable). We imputed missing data 10 times, performed the analysis over all the 10 imputations and averaged results using Rubin's rules (Rubin, 2004). Log-linearity of continuous variables was assessed visually by inspecting the shape of the distribution of the beta-estimates vs. the median by quintiles with regard to the outcome of interest (cluster 2). If deemed appropriate based on log-linearity, continuous variables were categorized. Variables with significant p-values (<0.05) in univariate analyses were considered in the multivariate model. Age and sex were "forced" in the model. The discrimination of the final multivariate model was assessed by calculating the area under the curve (AUC). Similar beta-estimates of variables in the multivariate model derived from the multiple imputation datasets were obtained when the pooled mean eGFR and E/E' were imputed in the original datasets (in N=23 and N=26 patients respectively; data not shown). Further analyses were therefore performed in the original dataset.

Thereafter, we studied which specific biomarkers were significantly associated with cluster 2 membership on top of the clinical multivariate model accounting for multiple comparisons using a Bonferroni adjusted p-value of <0.00014. To identify independent biomarkers, we subsequently excluded those correlated to each other (>0.3). Also here, from two correlated biomarkers, the biomarker with the largest mean absolute correlation was excluded.

The FHF-GKB complex network was queried in order to explore pathways and proteins that could connect together biomarker (BM) nodes of interest. Queries were expressed according to query patterns defining a path structure between two nodes such as

BM-BM and BM-pathway-BM, where the BM nodes are taken from a list of interest. The resulting graphs were merged in a figure illustrating all possible paths not longer than two edges, connecting BMs through pathways.

The association between cluster membership and the composite endpoint of CV death and/or CV hospitalizations (primary endpoint of MEDIA-DHF) within 1 year after inclusion in the study was studied using Kaplan–Meier estimates and Cox proportional hazards models. To derive clinical variables for adjustment, we constructed a clinical risk model (considering all aforementioned clinical variables) and used the variables that were significantly associated with the primary outcome in multivariate Cox regression as adjustment variables. Natriuretic peptides were included in the cluster analysis and therefore not included in the prognostic model. All significant clinical variables ($p < 0.05$) in univariate analysis were considered for the multivariate risk model. Age (per 10 years increase) and sex were “forced” in the model.

Statistical analyses were performed using SPSS 24 (IBM inc., Armonk, New York) and R (The R Foundation for Statistical Computing, Vienna, Austria).

Results

Cluster characteristics

The optimal number of clusters within this biomarker substudy of MEDIA-DHF was 2 (*Supplemental figure 2*). The distribution of demographic, clinical and echocardiographic variables according to the specific clusters is summarized in *Table 1*. Compared to cluster 1, patients in cluster 2 were older, more often had a recent episode of decompensated HF (<60 days), a previous HF hospitalization, atrial fibrillation, diabetes mellitus, peripheral arterial disease, NYHA class III/IV, complaints of fatigue on exertion, anemia, lower diastolic blood pressure, lower cholesterol measures (total cholesterol, LDL and HDL), worse renal function,

higher E/e', lower TAPSE and higher E/A. In addition, they were more often prescribed betablockers, loop or thiazide diuretics, oral anticoagulants, and insulin.

Clinical determinants of cluster 2 membership

Crude and adjusted odds ratios for the association between clinical variables and cluster 2 membership are listed in *Table 2*. There were four variables independently associated with cluster 2 membership: prescription of loop diuretics or betablockers, diabetes mellitus, and lower eGFR (= "clinical model").

Association between biomarkers and cluster 2 membership

For all individual biomarkers, associations with cluster 2 membership were assessed on top of the clinical model. A total of 17 biomarkers were identified (*Table 3*). These were: angiotensin-1 receptor (TIE2), ectonucleoside triphosphate diphosphohydrolase 2 (ENTPD2), eotaxin (CCL11), tumor necrosis factor ligand superfamily member 13B (TNFSF13B), platelet-derived growth factor C (PDGFC), L-selectin (SELL), proprotein convertase subtilisin/kexin type 9 (PCSK9), tumor necrosis factor (Ligand) superfamily member 12 (TWEAK), nitric oxide synthase (NOS3), granulysin (GNLY), E-selectin (SELE), serpin A9 (SERPINA9), azurocidin (AZU1), proto-oncogene tyrosine-protein kinase Src (SRC), adhesion G-protein coupled receptor G1 (ADGRG1), fibroblast growth factor 21 (FGF21) and growth hormone (GH). Addition of these 17 biomarkers to the clinical model significantly improved the multivariate model for the prediction of cluster 2 membership (AUC from 0.81 to 0.96). Distribution of the biomarkers according to the respective clusters is listed in *Supplemental table 4*.

Network analyses

Of the 17 cluster-associated protein biomarkers, 15 were linked with each other by known direct interactions or pathway-interactions linked to the immune system, signal transduction/cell interactions and metabolism (*Figure 1*).

Clinical risk model for cardiovascular outcome

Crude and adjusted hazard ratios for clinical variables associated with CV death and/or CV hospitalization are listed in *Supplemental table 5*. These variables were a history of CAD, pulmonary rales, age and sex.

Cluster outcomes

The composite endpoint of CV death and/or CV hospitalization occurred more often in cluster 2 compared to cluster 1 (resp. 20% (33/163) versus 12% (27/229), Log rank test: $p=0.024$; *Figure 2*). After adjustment for the clinical risk model, patients within cluster 2 had a significantly higher rate of CV death and/or CV hospitalizations than those in cluster 1 (adjusted hazard ratio 1.93, 95% CI 1.12-3.32, $p=0.017$). Adjusting on additional clinical variables in the model (such as previous HF hospitalization, diabetes mellitus, renal function, systolic blood pressure and different HF medication) did not change the significant association between cluster assignment and outcome (*Supplemental table 6*).

Discussion

The performance of unsupervised machine learning using data on >400 biomarkers in a large cohort of 392 HFpEF, otherwise well-characterized patients, led to the identification of 2 distinct HFpEF clusters. In addition to differences in clinical features and cardiovascular prognosis between clusters, we found 17 biomarkers to be significantly associated with cluster membership. This may indicate differences in pathophysiological mechanisms.

Differences between clusters: clinical features

Clinical variables that were significantly associated with cluster 2 membership were the prescription of loop diuretics or betablockers, diabetes mellitus, and lower eGFR. These have previously been associated with poor prognosis in HFpEF patients (Damman et al., 2014; Tribouilloy et al., 2008) and may indicate the presence of a cardiorenal syndrome as recently proposed (Zannad & Rossignol, 2018).

Differences between clusters: biomarkers and mechanistic significance

In this study, plasma levels of 17 biomarkers were significantly more elevated in cluster 2 compared to cluster 1. Network analysis revealed that these biomarkers may be grouped in 3 different mechanistic pathways: the immune system, signal transduction/cell interactions and metabolism. An overview of the biomarkers and their mechanistic significance is given in *Table 4*.

Other studies with smaller samples and fewer biomarkers found several biomarkers associated with outcome in HFpEF. In a sub study of Karolinska Rennes (KaRen), growth/differentiation factor-15 (GDF-15) was the strongest predictor for poor outcome (Hage et al., 2017), while Tromp *et al.* investigated 33 biomarkers in a cohort of HF patients and demonstrated that the remodeling marker osteopontin and the angiogenesis marker neuropilin predicted outcome (Tromp et al., 2017). Another study compared profiles of 92 biomarkers between HFrEF, HFmrEF and HFpEF patients and found that central proteins in HFpEF were integrin subunit beta-2 and catenin beta-1 (Tromp et al., 2018). A substudy of the Trial of Intensified versus standard Medical therapy in Elderly patients with Congestive Heart Failure (TIME-CHF) compared 15 biomarker from different pathways between HFrEF and HFpEF patients and found that markers of inflammation (hsCRP and cystatin C), fibrosis

(ST2) and anemia (hemoglobin) were more prominent in HFpEF than in HFrEF (Sanders-van Wijk et al., 2015). Interestingly, our results are novel since no overlap was present between the biomarkers that we found in our study and the biomarkers in other HFpEF studies (Hage et al., 2017; Santhanakrishnan et al., 2012; Tromp et al., 2017; Tromp et al., 2018). However, a common pathway of the biomarkers that were associated with poor prognosis in HFpEF patients in previous studies (Hage et al., 2017; Tromp et al., 2017) and our study seems to be the immune system. Our findings need to be confirmed by other studies investigating similar biomarkers.

Difference between clusters: cardiovascular outcome

In line with previous reports (Chioncel et al., 2017; Hwang, Melenovsky, & Borlaug, 2014; Vedin et al., 2017), we found that CAD and pulmonary rales were associated with poor outcome. Age and sex were kept in the models by their known prognostic value (Chioncel et al., 2017). After adjustment for these clinical variables, patients in cluster 2 had a worse cardiovascular outcome compared to the patients in cluster 1.

Clinical implications

This study may have clinical and research implications. More insight into the mechanisms related to poor outcome in HFpEF is obtained by the finding that the majority of the biomarkers associated with cluster 2 (the cluster with a higher risk for poor CV outcome) seem to be involved in processes related to the immune system, signal transduction cascades, cell interactions and metabolism. Our findings encourage additional studies investigating the underlying mechanisms and their clinical relevance. The biomarkers (and pathways) identified in this study may help select high-risk HFpEF patients which could be helpful for the inclusion or exclusion of patients in future trials. Moreover, our findings may be the basis

of investigating therapies specifically targeting these pathways and the potential use of corresponding markers potentially identifying patients with distinct mechanistic bioprofiles most likely to respond to the selected mechanistically targeted therapies. Such strategies could remediate the poor track record of past HFpEF large outcome trials (Rossignol et al., 2019).

Strengths and limitations

A strength of our study is that MEDIA-DHF was a large prospective European cohort in which data on >400 biomarkers from different disease domains were collected allowing for an unbiased approach to identify underlying pathophysiological pathways in HFpEF.

The most important limitation of this study is that we could not perform external validation of our prediction model due to the absence of other HFpEF cohorts with similar biomarkers, echocardiographic and follow up data. It is clear that other studies need to confirm our findings. Furthermore, at the time of enrollment, HFpEF was diagnosed following 2007 ESC diagnostic recommendations. Since the 2007 criteria, other criteria have been proposed and it has recently been shown that large variations in prevalence of diastolic dysfunction may be expected according to which criterion is used (Huttin et al., 2017).

However, when applying the H₂FPEF score by Reddy and colleagues (Reddy, Carter, Obokata, Redfield, & Borlaug, 2018) to the MEDIA-DHF cohort, only 2% of patients had a low probability of HFpEF whereas 58% and 40% of patients had an intermediate or high probability respectively. Third, the biomarker assay does not provide standard concentration units, making comparisons with clinically applied cut-offs difficult. Fourth, although the biomarker assay in this study covers a wide variety of disease domains, the possibility exists that other, now unmeasured, biomarkers may (also) play a role in the pathophysiology of HFpEF. Fifth, although it is biologically plausible that increased activation of processes related to, for example, the immune system may be associated with a poorer outcome in

HFpEF, it should be noted that reference values (from a healthy population) for most of the candidate biomarkers in this study are lacking. Sixth, although HFpEF is known to be a heterogeneous disease, the *NbClust* package identified only 2 clusters based on the available biomarker data. Including more (clinical) data may identify a larger number of clusters. Seventh, due to the observational nature of our study with only few CV events we did not study whether differences in treatment effects (for ACEi/ARBs, BBs, etc.) can be expected for the different clusters. Also, the low number of adverse events and small sample size preclude to obtain robust estimates. Last, our cohort consists of chronic and recently discharged HFpEF patients and results can therefore not be extrapolated to different (sicker) HFpEF populations.

Conclusion

Unsupervised learning algorithms applied to >400 biomarkers in a large cohort of 392 HFpEF patients led to the identification of 2 distinct HFpEF cluster phenotypes. In addition to differences in clinical features between clusters, we found 17 uncorrelated biomarkers with higher expression in cluster 2 compared to cluster 1. These biomarkers are involved in pathways linked to the immune system, signal transduction cascades, cell interactions and metabolism, that may contribute to different HFpEF phenotypes.

Clinical significance

- More insight is obtained in the mechanisms related to poor outcome in HFpEF patients since it was demonstrated that biomarkers associated with the high-risk cluster were related to the immune system, signal transduction cascades, cell interactions and metabolism
- Biomarkers (and pathways) identified in this study may help select high-risk HFpEF patients which could be helpful for the inclusion/exclusion of patients in future trials.
- Our findings may be the basis of investigating therapies specifically targeting these pathways and the potential use of corresponding markers potentially identifying patients with distinct mechanistic bioprofiles most likely to respond to the selected mechanistically targeted therapies.

Disclosures

This study was supported by a grant from the European Union (FP7-HEALTH-2010-MEDIA), by the French Programme Hospitalier de Recherche Clinique (PHRC) and by the RHU Fight-HF, a public grant overseen by the French National Research Agency (ANR) as part of the second “Investissements d’Avenir” program (reference: ANR-15-RHU-0004), the GEENAGE (ANR-15-IDEX-04-LUE) program, by the Contrat de Plan Etat Région Lorraine and FEDER IT2MP.) N-LA was supported by a Miguel Servet contract CP13/00221 from the “Instituto de Salud Carlos III-FEDER”. WJP and LvH were supported by CVON, Dutch Heart Foundation, The Hague, The Netherlands (RECONNECT and EARLY-HFpEF projects). AM received speaker's honoraria from Orion, Otsuka, Philips, Roche and Servier. AM received fees as member of advisory board and/or Steering Committee and/or research grant from Adrenomed, Epygon, Neurotronik, Roche, Sanofi and Sphingotec. AM owns shares in S-Form Pharma. SS acknowledges funding received from the European Society of Cardiology in form of an ESC Research Grant (R-2018-18686). SH was supported by IMI2-CARDIATEAM (N° 821508), research grants from the Netherlands Organization for Scientific Research (NOW; Vidi 91796338), the Netherlands Cardiovascular Research Initiative, an initiative with support of the Dutch Heart Foundation, CVON2016-Early HFPEF, 2015-10, CVON She-PREDICTS, grant 2017-21, CVON Arena-PRIME, 2017-18 and the ERA-Net-CVD project MacroERA, 01KL1706, and FWO G091018N.

Acknowledgments

We thank other colleagues for their important contributions to the MEDIA study in the participating centres, including the CRB Lorrain for the biobanking, Gabor Kunszt (Oslo University Hospital), Tamas Erdei and Julie Edwards (Cardiff University).

References

- Almontashiri, N. A., Vilmundarson, R. O., Ghasemzadeh, N., Dandona, S., Roberts, R., Quyyumi, A. A., . . . Stewart, A. F. (2014). Plasma PCSK9 levels are elevated with acute myocardial infarction in two independent retrospective angiographic studies. *PLoS One*, *9*(9), e106294. doi:10.1371/journal.pone.0106294
- Arcopinto, M., Salzano, A., Giallauria, F., Bossone, E., Isgaard, J., Marra, A. M., . . . Cittadini, A. (2017). Growth Hormone Deficiency Is Associated with Worse Cardiac Function, Physical Performance, and Outcome in Chronic Heart Failure: Insights from the T.O.S.C.A. GHD Study. *PLoS One*, *12*(1), e0170058. doi:10.1371/journal.pone.0170058
- Bayes-Genis, A., Nunez, J., Zannad, F., Ferreira, J. P., Anker, S. D., Cleland, J. G., . . . Voors, A. A. (2017). The PCSK9-LDL Receptor Axis and Outcomes in Heart Failure: BIostat-CHF Subanalysis. *J Am Coll Cardiol*, *70*(17), 2128-2136. doi:10.1016/j.jacc.2017.08.057
- Berezin, A. E., Kremzer, A. A., Martovitskaya, Y. V., Berezina, T. A., & Gromenko, E. A. (2016). Pattern of endothelial progenitor cells and apoptotic endothelial cell-derived microparticles in chronic heart failure patients with preserved and reduced left ventricular ejection fraction. *EBioMedicine*, *4*, 86-94. doi:10.1016/j.ebiom.2016.01.018
- Blanco-Colio, L. M. (2014). TWEAK/Fn14 Axis: A Promising Target for the Treatment of Cardiovascular Diseases. *Front Immunol*, *5*, 3. doi:10.3389/fimmu.2014.00003
- Brankovic, M., Martijn Akkerhuis, K., Mouthaan, H., Constantinescu, A., Caliskan, K., van Ramshorst, J., . . . Kardys, I. (2018). Utility of temporal profiles of new cardio-renal and pulmonary candidate biomarkers in chronic heart failure. *Int J Cardiol*. doi:10.1016/j.ijcard.2018.08.001
- Calderone, A., Castagnoli, L., & Cesareni, G. (2013). mentha: a resource for browsing integrated protein-interaction networks. *Nat Methods*, *10*(8), 690-691. doi:10.1038/nmeth.2561
- Chatr-Aryamontri, A., Oughtred, R., Boucher, L., Rust, J., Chang, C., Kolas, N. K., . . . Tyers, M. (2017). The BioGRID interaction database: 2017 update. *Nucleic Acids Res*, *45*(D1), D369-d379. doi:10.1093/nar/gkw1102
- Chen, H. N., Wang, D. J., Ren, M. Y., Wang, Q. L., & Sui, S. J. (2012). TWEAK/Fn14 promotes the proliferation and collagen synthesis of rat cardiac fibroblasts via the NF-small ka, CyrillicB pathway. *Mol Biol Rep*, *39*(8), 8231-8241. doi:10.1007/s11033-012-1671-3
- Chioncel, O., Lainscak, M., Seferovic, P. M., Anker, S. D., Crespo-Leiro, M. G., Harjola, V. P., . . . Filippatos, G. (2017). Epidemiology and one-year outcomes in patients with chronic heart failure and preserved, mid-range and reduced ejection fraction: an analysis of the ESC Heart Failure Long-Term Registry. *Eur J Heart Fail*, *19*(12), 1574-1585. doi:10.1002/ejhf.813
- Chong, A. Y., Caine, G. J., Freestone, B., Blann, A. D., & Lip, G. Y. (2004). Plasma angiopoietin-1, angiopoietin-2, and angiopoietin receptor tie-2 levels in congestive heart failure. *J Am Coll Cardiol*, *43*(3), 423-428. doi:10.1016/j.jacc.2003.08.042
- Czucz, J., Cervenak, L., Forhecz, Z., Gombos, T., Pozsonyi, Z., Kunde, J., . . . Prohaszka, Z. (2011). Serum soluble E-selectin and NT-proBNP levels additively predict mortality in diabetic patients with chronic heart failure. *Clin Res Cardiol*, *100*(7), 587-594. doi:10.1007/s00392-011-0283-6
- Damman, K., Valente, M. A., Voors, A. A., O'Connor, C. M., van Veldhuisen, D. J., & Hillege, H. L. (2014). Renal impairment, worsening renal function, and outcome in patients with heart failure: an updated meta-analysis. *Eur Heart J*, *35*(7), 455-469. doi:10.1093/eurheartj/ehs386
- Dankiewicz, J., Linder, A., Annborn, M., Rundgren, M., & Friberg, H. (2013). Heparin-binding protein: an early indicator of critical illness and predictor of outcome in cardiac arrest. *Resuscitation*, *84*(7), 935-939. doi:10.1016/j.resuscitation.2013.01.006
- Dehm, S. M., & Bonham, K. (2004). SRC gene expression in human cancer: the role of transcriptional activation. *Biochem Cell Biol*, *82*(2), 263-274. doi:10.1139/o03-077
- Diny, N. L., Hou, X., Barin, J. G., Chen, G., Talor, M. V., Schaub, J., . . . Cihakova, D. (2016). Macrophages and cardiac fibroblasts are the main producers of eotaxins and regulate eosinophil trafficking to the heart. *Eur J Immunol*, *46*(12), 2749-2760. doi:10.1002/eji.201646557
- Economou, E., Tousoulis, D., Katinioti, A., Stefanadis, C., Trikas, A., Pitsavos, C., . . . Toutouzas, P. (2001). Chemokines in patients with ischaemic heart disease and the effect of coronary angioplasty. *Int J Cardiol*, *80*(1), 55-60.
- Fabregat, A., Jupe, S., Matthews, L., Sidiropoulos, K., Gillespie, M., Garapati, P., . . . D'Eustachio, P. (2018). The Reactome Pathway Knowledgebase. *Nucleic Acids Res*, *46*(D1), D649-d655. doi:10.1093/nar/gkx1132
- Ferraccioli, G., & Gremese, E. (2017). B cell activating factor (BAFF) and BAFF receptors: fakes and facts. *Clin Exp Immunol*, *190*(3), 291-292. doi:10.1111/cei.13039
- Franssen, C., Chen, S., Unger, A., Korkmaz, H. I., De Keulenaer, G. W., Tschope, C., . . . Hamdani, N. (2016). Myocardial Microvascular Inflammatory Endothelial Activation in Heart Failure With Preserved Ejection Fraction. *JACC Heart Fail*, *4*(4), 312-324. doi:10.1016/j.jchf.2015.10.007
- Frazer, J. K., Jackson, D. G., Gaillard, J. P., Lutter, M., Liu, Y. J., Banchereau, J., . . . Pascual, V. (2000). Identification of centerin: a novel human germinal center B cell-restricted serpin. *Eur J Immunol*, *30*(10), 3039-3048. doi:10.1002/1521-4141(200010)30:10<3039::aid-immu3039>3.0.co;2-h

- Gautam, N., Olofsson, A. M., Herwald, H., Iversen, L. F., Lundgren-Akerlund, E., Hedqvist, P., . . . Lindbom, L. (2001). Heparin-binding protein (HBP/CAP37): a missing link in neutrophil-evoked alteration of vascular permeability. *Nat Med*, 7(10), 1123-1127. doi:10.1038/nm1001-1123
- Hage, C., Michaelsson, E., Linde, C., Donal, E., Daubert, J. C., Gan, L. M., & Lund, L. H. (2017). Inflammatory Biomarkers Predict Heart Failure Severity and Prognosis in Patients With Heart Failure With Preserved Ejection Fraction: A Holistic Proteomic Approach. *Circ Cardiovasc Genet*, 10(1). doi:10.1161/circgenetics.116.001633
- Hamann, J., Aust, G., Arac, D., Engel, F. B., Formstone, C., Fredriksson, R., . . . Schioth, H. B. (2015). International Union of Basic and Clinical Pharmacology. XCIV. Adhesion G protein-coupled receptors. *Pharmacol Rev*, 67(2), 338-367. doi:10.1124/pr.114.009647
- He, Q., & LaPointe, M. C. (2001). Src and Rac mediate endothelin-1 and lysophosphatidic acid stimulation of the human brain natriuretic peptide promoter. *Hypertension*, 37(2 Pt 2), 478-484.
- Huang, K. Y., & Lin, H. H. (2018). The Activation and Signaling Mechanisms of GPR56/ADGRG1 in Melanoma Cell. *Front Oncol*, 8, 304. doi:10.3389/fonc.2018.00304
- Huang, R. B., & Eniola-Adefeso, O. (2012). Shear stress modulation of IL-1beta-induced E-selectin expression in human endothelial cells. *PLoS One*, 7(2), e31874. doi:10.1371/journal.pone.0031874
- Huttin, O., Fraser, A. G., Coiro, S., Bozec, E., Selton-Suty, C., Lamiral, Z., . . . Girerd, N. (2017). Impact of Changes in Consensus Diagnostic Recommendations on the Echocardiographic Prevalence of Diastolic Dysfunction. *J Am Coll Cardiol*, 69(25), 3119-3121. doi:10.1016/j.jacc.2017.04.039
- Hwang, S. J., Melenovsky, V., & Borlaug, B. A. (2014). Implications of coronary artery disease in heart failure with preserved ejection fraction. *J Am Coll Cardiol*, 63(25 Pt A), 2817-2827. doi:10.1016/j.jacc.2014.03.034
- Ikezoe, K., Ohshima, S., Osoegawa, M., Tanaka, M., Ogawa, K., Nagata, K., & Kira, J. I. (2006). Expression of granulysin in polymyositis and inclusion-body myositis. *J Neurol Neurosurg Psychiatry*, 77(10), 1187-1190. doi:10.1136/jnnp.2005.081810
- Ivetic, A. (2018). A head-to-tail view of L-selectin and its impact on neutrophil behaviour. *Cell Tissue Res*, 371(3), 437-453. doi:10.1007/s00441-017-2774-x
- Jones, G. T., Phillips, L. V., Williams, M. J., van Rij, A. M., & Kabir, T. D. (2016). Two C-C Family Chemokines, Eotaxin and RANTES, Are Novel Independent Plasma Biomarkers for Abdominal Aortic Aneurysm. *J Am Heart Assoc*, 5(5). doi:10.1161/jaha.115.002993
- Kao, D. P., Lewsey, J. D., Anand, I. S., Massie, B. M., Zile, M. R., Carson, P. E., . . . Lindenfeld, J. (2015). Characterization of subgroups of heart failure patients with preserved ejection fraction with possible implications for prognosis and treatment response. *Eur J Heart Fail*, 17(9), 925-935. doi:10.1002/ehf.327
- Kibbe, W. A., Arze, C., Felix, V., Mitraka, E., Bolton, E., Fu, G., . . . Schriml, L. M. (2015). Disease Ontology 2015 update: an expanded and updated database of human diseases for linking biomedical knowledge through disease data. *Nucleic Acids Res*, 43(Database issue), D1071-1078. doi:10.1093/nar/gku1011
- Kotsch, K., Mashreghi, M. F., Bold, G., Tretow, P., Beyer, J., Matz, M., . . . Reinke, P. (2004). Enhanced granulysin mRNA expression in urinary sediment in early and delayed acute renal allograft rejection. *Transplantation*, 77(12), 1866-1875.
- Kumar, J., Okada, S., Clayberger, C., & Krensky, A. M. (2001). Granulysin: a novel antimicrobial. *Expert Opin Investig Drugs*, 10(2), 321-329. doi:10.1517/13543784.10.2.321
- Lee, K. W., Lip, G. Y., & Blann, A. D. (2004). Plasma angiotensin-1, angiotensin-2, angiotensin receptor tie-2, and vascular endothelial growth factor levels in acute coronary syndromes. *Circulation*, 110(16), 2355-2360. doi:10.1161/01.cir.0000138112.90641.7f
- Li, X., Tjwa, M., Moons, L., Fons, P., Noel, A., Ny, A., . . . Carmeliet, P. (2005). Revascularization of ischemic tissues by PDGF-CC via effects on endothelial cells and their progenitors. *J Clin Invest*, 115(1), 118-127. doi:10.1172/jci19189
- Linder, A., Akesson, P., Inghammar, M., Treutiger, C. J., Linner, A., & Sundén-Cullberg, J. (2012). Elevated plasma levels of heparin-binding protein in intensive care unit patients with severe sepsis and septic shock. *Crit Care*, 16(3), R90. doi:10.1186/cc11353
- Linder, A., Soehnlein, O., & Akesson, P. (2010). Roles of heparin-binding protein in bacterial infections. *J Innate Immun*, 2(5), 431-438. doi:10.1159/000314853
- Lu, D., & Insel, P. A. (2013). Hydrolysis of extracellular ATP by ectonucleoside triphosphate diphosphohydrolase (ENTPD) establishes the set point for fibrotic activity of cardiac fibroblasts. *J Biol Chem*, 288(26), 19040-19049. doi:10.1074/jbc.M113.466102
- Lundberg, M., Eriksson, A., Tran, B., Assarsson, E., & Fredriksson, S. (2011). Homogeneous antibody-based proximity extension assays provide sensitive and specific detection of low-abundant proteins in human blood. *Nucleic Acids Res*, 39(15), e102. doi:10.1093/nar/gkr424
- Luo, R., Jeong, S. J., Jin, Z., Strokes, N., Li, S., & Piao, X. (2011). G protein-coupled receptor 56 and collagen III, a receptor-ligand pair, regulates cortical development and lamination. *Proc Natl Acad Sci U S A*, 108(31), 12925-12930. doi:10.1073/pnas.1104821108
- Ma, X. L., Weyrich, A. S., Lefer, D. J., Buerke, M., Albertine, K. H., Kishimoto, T. K., & Lefer, A. M. (1993). Monoclonal antibody to L-selectin attenuates neutrophil accumulation and protects ischemic reperfused cat myocardium. *Circulation*, 88(2), 649-658.
- Medamana, J., Clark, R. A., & Butler, J. (2017). Platelet-Derived Growth Factor in Heart Failure. *Handb Exp Pharmacol*, 243, 355-369. doi:10.1007/164_2016_80

- Moreno, H., Jr., Metze, K., Bento, A. C., Antunes, E., Zatz, R., & de Nucci, G. (1996). Chronic nitric oxide inhibition as a model of hypertensive heart muscle disease. *Basic Res Cardiol*, *91*(3), 248-255.
- Morrison, A. C., Bare, L. A., Luke, M. M., Pankow, J. S., Mosley, T. H., Devlin, J. J., . . . Boerwinkle, E. (2008). Single nucleotide polymorphisms associated with coronary heart disease predict incident ischemic stroke in the atherosclerosis risk in communities study. *Cerebrovasc Dis*, *26*(4), 420-424. doi:10.1159/000155637
- Nagasawa, M., Ogawa, K., Imashuku, S., & Mizutani, S. (2007). Serum granulysin is elevated in patients with hemophagocytic lymphohistiocytosis. *Int J Hematol*, *86*(5), 470-473. doi:10.1532/ijh97.07084
- Ong, K. L., Hui, N., Januszewski, A. S., Kaakoush, N. O., Xu, A., Fayyad, R., . . . Rye, K. A. (2019). High plasma FGF21 levels predicts major cardiovascular events in patients treated with atorvastatin (from the Treating to New Targets [TNT] Study). *Metabolism*, *93*, 93-99. doi:10.1016/j.metabol.2018.11.006
- Ornitz, D. M., & Itoh, N. (2015). The Fibroblast Growth Factor signaling pathway. *Wiley Interdiscip Rev Dev Biol*, *4*(3), 215-266. doi:10.1002/wdev.176
- Pardo, J., Perez-Galan, P., Gamen, S., Marzo, I., Monleon, I., Kaspar, A. A., . . . Anel, A. (2001). A role of the mitochondrial apoptosis-inducing factor in granulysin-induced apoptosis. *J Immunol*, *167*(3), 1222-1229.
- Paulus, W. J., Tschope, C., Sanderson, J. E., Rusconi, C., Flachskampf, F. A., Rademakers, F. E., . . . Brutsaert, D. L. (2007). How to diagnose diastolic heart failure: a consensus statement on the diagnosis of heart failure with normal left ventricular ejection fraction by the Heart Failure and Echocardiography Associations of the European Society of Cardiology. *Eur Heart J*, *28*(20), 2539-2550. doi:10.1093/eurheartj/ehm037
- Persic, V., Ruzic, A., Miletic, B., Samsa, D. T., Rakic, M., Rajjevic, D., . . . Laskarin, G. (2012). Granulysin Expression in Lymphocytes that Populate the Peripheral Blood and the Myocardium after an Acute Coronary Event. *Scand J Immunol*, *75*(2), 231-242. doi:10.1111/j.1365-3083.2011.02646.x
- Pinero, J., Bravo, A., Queralt-Rosinach, N., Gutierrez-Sacristan, A., Deu-Pons, J., Centeno, E., . . . Furlong, L. I. (2017). DisGeNET: a comprehensive platform integrating information on human disease-associated genes and variants. *Nucleic Acids Res*, *45*(D1), D833-d839. doi:10.1093/nar/gkw943
- Ponikowski, P., Voors, A. A., Anker, S. D., Bueno, H., Cleland, J. G. F., Coats, A. J. S., . . . van der Meer, P. (2016). 2016 ESC Guidelines for the diagnosis and treatment of acute and chronic heart failure: The Task Force for the diagnosis and treatment of acute and chronic heart failure of the European Society of Cardiology (ESC) Developed with the special contribution of the Heart Failure Association (HFA) of the ESC. *Eur Heart J*, *37*(27), 2129-2200. doi:10.1093/eurheartj/ehw128
- Ptaszynska-Kopczynska, K., Marcinkiewicz-Siemion, M., Lisowska, A., Waszkiewicz, E., Witkowski, M., Jasiewicz, M., . . . Kaminski, K. A. (2016). Alterations of soluble TWEAK and CD163 concentrations in patients with chronic heart failure. *Cytokine*, *80*, 7-12. doi:10.1016/j.cyto.2016.02.005
- Reddy, Y. N. V., Carter, R. E., Obokata, M., Redfield, M. M., & Borlaug, B. A. (2018). A Simple, Evidence-Based Approach to Help Guide Diagnosis of Heart Failure With Preserved Ejection Fraction. *Circulation*, *138*(9), 861-870. doi:10.1161/circulationaha.118.034646
- Rosignol P, Hernandez AF, Solomon S, Zannad F. Heart failure drug treatment. (2019). *Lancet*, *in press*.
- Rubin, D. B. (2004). *Multiple Imputation for Nonresponse in Surveys*. New York: John Wiley and Sons.
- Sabatine, M. S., Giugliano, R. P., Keech, A. C., Honarpour, N., Wiviott, S. D., Murphy, S. A., . . . Pedersen, T. R. (2017). Evolocumab and Clinical Outcomes in Patients with Cardiovascular Disease. *N Engl J Med*, *376*(18), 1713-1722. doi:10.1056/NEJMoa1615664
- Salzano, A., Marra, A. M., Ferrara, F., Arcopinto, M., Bobbio, E., Valente, P., . . . Cittadini, A. (2016). Multiple hormone deficiency syndrome in heart failure with preserved ejection fraction. *Int J Cardiol*, *225*, 1-3. doi:10.1016/j.ijcard.2016.09.085
- Salzano, A., Marra, A. M., D'Assante, R., Arcopinto, M., Suzuki, T., Bossone, E., & Cittadini, A. (2018). Growth Hormone Therapy in Heart Failure. *Heart Fail Clin*, *14*(4), 501-515. doi:10.1016/j.hfc.2018.05.002
- Sanchez-Martinez, S., Duchateau, N., Erdei, T., Kunszt, G., Aakhus, S., Degiovanni, A., . . . Bijnens, B. H. (2018). Machine Learning Analysis of Left Ventricular Function to Characterize Heart Failure With Preserved Ejection Fraction. *Circ Cardiovasc Imaging*, *11*(4), e007138. doi:10.1161/circimaging.117.007138
- Sanders-van Wijk, S., van Empel, V., Davarzani, N., Maeder, M. T., Handschin, R., Pfisterer, M. E., & Brunner-La Rocca, H. P. (2015). Circulating biomarkers of distinct pathophysiological pathways in heart failure with preserved vs. reduced left ventricular ejection fraction. *Eur J Heart Fail*, *17*(10), 1006-1014. doi:10.1002/ejhf.414
- Santhanakrishnan, R., Chong, J. P., Ng, T. P., Ling, L. H., Sim, D., Leong, K. T., . . . Lam, C. S. (2012). Growth differentiation factor 15, ST2, high-sensitivity troponin T, and N-terminal pro brain natriuretic peptide in heart failure with preserved vs. reduced ejection fraction. *Eur J Heart Fail*, *14*(12), 1338-1347. doi:10.1093/eurjhf/hfs130
- Sevigny, J., Sundberg, C., Braun, N., Guckelberger, O., Csizmadia, E., Qawi, I., . . . Robson, S. C. (2002). Differential catalytic properties and vascular topography of murine nucleoside triphosphate diphosphohydrolase 1 (NTPDase1) and NTPDase2 have implications for thromboregulation. *Blood*, *99*(8), 2801-2809.
- Shah, S. J., Katz, D. H., Selvaraj, S., Burke, M. A., Yancy, C. W., Gheorghide, M., . . . Deo, R. C. (2015). Phenomapping for novel classification of heart failure with preserved ejection fraction. *Circulation*, *131*(3), 269-279. doi:10.1161/circulationaha.114.010637
- Shimada, Y. J., & Cannon, C. P. (2015). PCSK9 (Proprotein convertase subtilisin/kexin type 9) inhibitors: past, present, and the future. *Eur Heart J*, *36*(36), 2415-2424. doi:10.1093/eurheartj/ehv174

- Slenter, D. N., Kutmon, M., Hanspers, K., Riutta, A., Windsor, J., Nunes, N., . . . Willighagen, E. L. (2018). WikiPathways: a multifaceted pathway database bridging metabolomics to other omics research. *Nucleic Acids Res*, *46*(D1), D661-d667. doi:10.1093/nar/gkx1064
- Smith, T. L., Van Slyke, P., Jones, N., Dumont, D. J., & McGlade, C. J. (2018). Tie2 signalling through Erk1/2 regulates TLR4 driven inflammation. *Cell Signal*, *51*, 211-221. doi:10.1016/j.cellsig.2018.08.001
- Stein, B., Eschenhagen, T., Rudiger, J., Scholz, H., Forstermann, U., & Gath, I. (1998). Increased expression of constitutive nitric oxide synthase III, but not inducible nitric oxide synthase II, in human heart failure. *J Am Coll Cardiol*, *32*(5), 1179-1186.
- Szklarczyk, D., Franceschini, A., Wyder, S., Forslund, K., Heller, D., Huerta-Cepas, J., . . . von Mering, C. (2015). STRING v10: protein-protein interaction networks, integrated over the tree of life. *Nucleic Acids Res*, *43*(Database issue), D447-452. doi:10.1093/nar/gku1003
- Tabassian, M., Sunderji, I., Erdei, T., Sanchez-Martinez, S., Degiovanni, A., Marino, P., . . . D'Hooge, J. (2018). Diagnosis of Heart Failure With Preserved Ejection Fraction: Machine Learning of Spatiotemporal Variations in Left Ventricular Deformation. *J Am Soc Echocardiogr*, *31*(12), 1272-1284.e1279. doi:10.1016/j.echo.2018.07.013
- Tribouilloy, C., Rusinaru, D., Mahjoub, H., Souliere, V., Levy, F., Peltier, M., . . . Massy, Z. (2008). Prognosis of heart failure with preserved ejection fraction: a 5 year prospective population-based study. *Eur Heart J*, *29*(3), 339-347. doi:10.1093/eurheartj/ehm554
- Tromp, J., Khan, M. A., Klip, I. T., Meyer, S., de Boer, R. A., Jaarsma, T., . . . Voors, A. A. (2017). Biomarker Profiles in Heart Failure Patients With Preserved and Reduced Ejection Fraction. *J Am Heart Assoc*, *6*(4). doi:10.1161/jaha.116.003989
- Tromp, J., Westenbrink, B. D., Ouwerkerk, W., van Veldhuisen, D. J., Samani, N. J., Ponikowski, P., . . . Voors, A. A. (2018). Identifying Pathophysiological Mechanisms in Heart Failure With Reduced Versus Preserved Ejection Fraction. *J Am Coll Cardiol*, *72*(10), 1081-1090. doi:10.1016/j.jacc.2018.06.050
- Tsao, C. W., Lyass, A., Enserro, D., Larson, M. G., Ho, J. E., Kizer, J. R., . . . Vasan, R. S. (2018). Temporal Trends in the Incidence of and Mortality Associated With Heart Failure With Preserved and Reduced Ejection Fraction. *JACC Heart Fail*, *6*(8), 678-685. doi:10.1016/j.jchf.2018.03.006
- Tsiantoulas, D., Sage, A. P., Goderle, L., Ozsvar-Kozma, M., Murphy, D., Porsch, F., . . . Binder, C. J. (2018). B Cell-Activating Factor Neutralization Aggravates Atherosclerosis. *Circulation*, *138*(20), 2263-2273. doi:10.1161/circulationaha.117.032790
- UniProt: the universal protein knowledgebase. (2017). *Nucleic Acids Res*, *45*(D1), D158-d169. doi:10.1093/nar/gkw1099
- Vedin, O., Lam, C. S. P., Koh, A. S., Benson, L., Teng, T. H. K., Tay, W. T., . . . Lund, L. H. (2017). Significance of Ischemic Heart Disease in Patients With Heart Failure and Preserved, Midrange, and Reduced Ejection Fraction: A Nationwide Cohort Study. *Circ Heart Fail*, *10*(6). doi:10.1161/circheartfailure.117.003875
- Vitello, A. M., Du, Y., Buttrick, P. M., & Walker, L. A. (2012). Serendipitous discovery of a novel protein signaling mechanism in heart failure. *Biochem Biophys Res Commun*, *421*(3), 431-435. doi:10.1016/j.bbrc.2012.03.124
- Williams, T. J. (2015). Eotaxin-1 (CCL11). *Front Immunol*, *6*, 84. doi:10.3389/fimmu.2015.00084
- Woo, Y. C., Xu, A., Wang, Y., & Lam, K. S. (2013). Fibroblast growth factor 21 as an emerging metabolic regulator: clinical perspectives. *Clin Endocrinol (Oxf)*, *78*(4), 489-496. doi:10.1111/cen.12095
- Zannad, F., & Rossignol, P. (2018). Cardiorenal Syndrome Revisited. *Circulation*, *138*(9), 929-944. doi:10.1161/circulationaha.117.028814
- Zouggari, Y., Ait-Oufella, H., Bonnin, P., Simon, T., Sage, A. P., Guerin, C., . . . Mallat, Z. (2013). B lymphocytes trigger monocyte mobilization and impair heart function after acute myocardial infarction. *Nat Med*, *19*(10), 1273-1280. doi:10.1038/nm.3284
- Zymek, P., Bujak, M., Chatila, K., Cieslak, A., Thakker, G., Entman, M. L., & Frangogiannis, N. G. (2006). The role of platelet-derived growth factor signaling in healing myocardial infarcts. *J Am Coll Cardiol*, *48*(11), 2315-2323. doi:10.1016/j.jacc.2006.07.060

Table 1 Baseline characteristics of patients according to clusters

	Cluster 1 (N=229)	Cluster 2 (N=163)	p-value	Percentage missing
Female sex, n (%)	152 (66%)	98 (60%)	0.2	0%
Age, years, median (IQR)	73 (66-79)	76 (69-82)	<0.001	0%
Recently decompensated chronic HF, n (%)	27 (12%)	33 (20%)	0.022	0%
Smoking status, n (%)				1%
Never	127 (56%)	78 (48%)	0.16	
Former	79 (35%)	71 (44%)		
Current	22 (10%)	12 (8%)		
Alcohol consumption, n (%)				1%
Non-consumer	144 (63%)	101 (64%)	0.4	
1-2 drinks/day	76 (33%)	48 (30%)		
>2 drinks/day	8 (4%)	10 (6%)		
BMI, kg/m ² , mean±SD	30.5±5.7	30.7±6.8	0.76	1%
Waist circumference, cm, mean±SD	103.7±13.0	106.4±15.3	0.094	21%
SBP, mmHg, mean±SD	138±21	136±26	0.32	2%
DBP, mmHg, mean±SD	76±11	72±12	0.002	2%
Pulmonary rales, n (%)	50 (22%)	39 (25%)	0.51	1%
NYHA class III/IV, n (%)	32 (14%)	41 (25%)	0.005	0%
Peripheral edema, n (%)	96 (42 %)	82 (50%)	0.1	1%
Jugular venous distension, n (%)	10 (5%)	14 (9%)	0.088	3%
Hepatomegaly, n (%)	8 (4%)	5 (3%)	0.78	7%
Fatigue on exertion, n (%)	170 (76%)	135 (84%)	0.036	2%
Heart rate, bmp, mean±SD	69±15	71±14	0.21	3%
Previous HF hospitalization, n (%)	65 (29%)	72 (45%)	0.001	2%
Atrial fibrillation, n (%)	53 (24%)	64 (40%)	<0.001	3%
Hypertension, n (%)	195 (86%)	147 (91%)	0.12	1%
Diabetes mellitus, n (%)	79 (35%)	75 (46%)	0.021	0%
Coronary artery disease, n (%)	68 (31%)	60 (38%)	0.14	3%
Stroke or TIA, n (%)	28 (12%)	16 (10%)	0.47	1%
Peripheral artery disease, n (%)	13 (6%)	21 (13%)	0.013	2%
COPD, n (%)	38 (17%)	33 (21%)	0.34	2%
Laboratory measurements, mean±SD				
Total cholesterol, mg/dL	181±39	168±48	0.015	17%
LDLc, mg/dL	103.2±33.78	94.1±41.4	0.042	20%
HDLc, mg/dL	56.8±22.1	48.7±14.0	<0.001	19%
Hb, g/dL	13.3±1.5	12.6±1.8	<0.001	12%
Anemia, n (%)	72 (35%)	71 (50%)	0.005	12%
eGFR, mL/min/1.73m ²	76.3±20.4	52.6±21.4	<0.001	6%
Medication prescription rates, n (%)				
ACEi or ARB	192 (84%)	127 (78%)	0.15	0%
Betablockers	154 (67%)	132 (81%)	0.003	0%

Loop diuretics	107 (47%)	128 (79%)	<0.001	0%
Thiazide diuretics	61 (27%)	26 (16%)	0.013	0%
MRA	20 (9%)	23 (14%)	0.096	0%
Aspirin	94 (41%)	65 (40%)	0.82	0%
Oral anticoagulants	78 (34%)	83 (51%)	<0.001	0%
Insulin	22 (10%)	30 (18%)	0.012	0%
Statin	139 (61%)	102 (63%)	0.71	0%
Echocardiographic parameters, mean±SD				
e'	7.2±2.1	7.5±2.1	0.18	7%
E/e'	12.7±4.6	14.2±5.9	0.008	7%
LVEF, %	61.2±7.1	60.2±6.7	0.15	0%
PASP, mmHg	32.6±12.5	38.0±12.4	<0.001	25%
TAPSE, cm	21.4±4.5	19.2±4.9	<0.001	10%
E/A	1.1±0.6	1.5±1.1	<0.001	30%

Legend: HF, heart failure; BMI, body mass index; DM, diabetes mellitus; CAD, coronary artery disease; PAD, peripheral artery disease; COPD, chronic obstructive pulmonary disease; OSAS, obstructive sleep apnea syndrome; TIA, transient ischemic attack; DBP, diastolic blood pressure; SBP, systolic blood pressure; NYHA, New York Heart Association; eGFR, estimated glomerular filtration rate; BNP, brain natriuretic peptide; NT-proBNP, N-terminal pro-brain natriuretic peptide; ASA, acetylsalicylic acid; ACEi, ACE-inhibitor; ARB, angiotensin receptor blocker; BB, betablocker; MRA, mineralocorticoid receptor antagonist; LVEF, left ventricular ejection fraction; E/e', the ratio of mitral inflow velocity and early mitral annulus velocity, PASP, pulmonary artery systolic pressure; TAPSE, Tricuspid Annular Plane Systolic Excursion; E/A, ratio of the early (E) to late (A) ventricular filling velocities; IQR, interquartile range.

Anemia is defined following the definition of the World Health Organization (<12 g/dL in females and <13 g/dL in males)

Table 2 Crude and adjusted odds ratios for the association between clinical variables and cluster membership

Set of clinical variables associated with cluster 2 membership	Univariate analyses		Multivariate analyses	
	OR (95% CI)	p-value	OR (95% CI)	p-value
Loop diuretics	4.17 (2.65-6.57)	<0.001	2.36 (1.41-3.95)	0.001
Betablockers	2.07 (1.29-3.35)	0.003	1.86 (1.06-3.28)	0.031
Diabetes mellitus	1.62 (1.07-2.44)	0.022	1.69 (1.02-2.82)	0.042
eGFR, per 1 mL/min/1.73m ² increase	0.95 (0.93-0.96)	<0.001	0.95 (0.94-0.97)	<0.001
Female sex	0.76 (0.50-1.16)	0.21	0.77 (0.46-1.27)	0.30
Age, per year increase	1.04 (1.02-1.07)	<0.001	1.02 (0.99-1.05)	0.17

Legend: eGFR, estimated glomerular filtration rate; OR, odds ratio; CI, confidence interval; AUC, area under the curve. Age & sex were “forced” in the model.

Table 3 Multiple testing-corrected and uncorrelated (Pearson correlation <0.3) biomarkers associated with cluster 2 membership on top of the clinical model

	Bivariate logistic regression analyses	
	<i>OR (95% CI)</i>	<i>p-value</i>
TIE2	19.83 (6.53-60.23)	<0.001
ENTPD2	13.21 (4.12-42.36)	<0.001
CCL11	6.44 (3.15-13.17)	<0.001
TNFSF13B	5.39 (2.79-10.41)	<0.001
PDGFC	5.09 (2.27-11.39)	<0.001
SELL	4.47 (2.42-9.28)	<0.001
PCSK9	4.04 (2.14-7.62)	<0.001
TWEAK	4.00 (2.02-7.94)	<0.001
NOS3	3.46 (2.14-5.62)	<0.001
GNLY	3.45 (1.89-6.29)	<0.001
SELE	2.43 (1.65-3.58)	<0.001
SERPINA9	2.17 (1.49-3.16)	<0.001
AZU1	1.87 (1.42-2.45)	<0.001
SRC	1.63 (1.29-2.05)	<0.001
ADGRG1	1.55 (1.26-1.91)	<0.001
FGF-21	1.49 (1.23-1.79)	<0.001
GH	1.34 (1.16-1.56)	<0.001

Legend: TIE2, angiopoietin-1 receptor; ENTPD2, ectonucleoside triphosphate diphosphohydrolase 2; CCL11, eotaxin; TNFSF13B, tumor necrosis factor ligand superfamily member 13B; PDGFC, platelet-derived growth factor C; SELL, L-selectin; PCSK9, proprotein convertase subtilisin/kexin type 9; TWEAK, tumor necrosis factor (Ligand) superfamily, member 12; NOS3, nitric oxide synthase; GNLY, granulysin; SELE, E-selectine; SERPINA9, serpin A9; AZU1, azurocidin; SRC, Proto-oncogene tyrosine-protein kinase Src; ADGRG1, adhesion G-protein coupled receptor G1; FGF_21_1, fibroblast growth factor 21; GH, growth hormone.

Table 4 Overview of the mechanistic significance of biomarkers that were more highly expressed in patients in cluster 2 than in cluster 1

Individual biomarker	Mechanistic significance	Previous relevant reports	
		Basic reports	Clinical reports
<i>Immune system</i>			
TWEAK	Belongs to the TNF receptor superfamily and regulates several cell functions such as proliferation, apoptosis, inflammation, angiogenesis, and collagen synthesis in cardiac fibroblasts(Blanco-Colio, 2014)(Chen, Wang, Ren, Wang, & Sui, 2012; Ptaszynska-Kopczynska et al., 2016)		Increased in HFREF(Ptaszynska-Kopczynska et al., 2016). No study in HFPEF
TNFSF13B	Member of the TNF superfamily. Regulates B- and T-cell function(Ferraccioli & Gremese, 2017)	A key driver of coronary heart disease and aggravates atherosclerosis(Tsiantoulas et al., 2018)	High levels associated with poor prognosis in MI(Zougari et al., 2013)
GNLY	Antimicrobial protein present in the granules of cytotoxic T lymphocytes and natural killer cells(Kumar, Okada, Clayberger, & Krensky, 2001) and involved in apoptosis(Pardo et al., 2001)		Increased in infection, auto-immune disease and after NSTEMI (Ikezoe et al., 2006; Kotsch et al., 2004; Nagasawa, Ogawa, Imashuku, & Mizutani, 2007; Persic et al., 2012)
AZU1	Stored in neutrophil granules. Acts as an inflammatory mediator inducing endothelial leakage(Gautam et al., 2001; Linder, Soehnlein, & Akesson, 2010)		Early indicator of organ dysfunction after infection (Linder et al., 2012) and cardiac arrest(Dankiewicz, Linder, Annborn, Rundgren, & Friberg, 2013). Serial measurements predicted poor outcome in chronic HF(Brankovic et al., 2018)
CCL11	Eosinophil chemoattractant	Plays a role in the pathogenesis of several allergic conditions (e.g. asthma)(Williams, 2015)	Increased in eosinophilic myocarditis(Diny et al., 2016), abdominal aortic aneurysms (Jones, Phillips, Williams, van Rij, & Kabir, 2016) and CAD (Economou et al., 2001).

NOS3	Enzyme that synthesizes nitric oxide, primarily in the vascular endothelium	Inhibition promotes hypertension and causes cardiac ischemia in rats(Moreno et al., 1996)	Increased expression in ventricular myocardium of end-stage dilated, ischemic and postmyocarditis CMP (Stein et al., 1998)
SERPINA9	Maturation and maintenance of b-cells (Frazer et al., 2000)		SNPs in the SERPINA9 gene have been associated with incident CAD and ischemic stroke (Morrison et al., 2008). No studies in HF.
SELL	Cell surface adhesion protein which mediates the adherence of lymphocytes to endothelial cells(Ivetic, 2018)	Inhibition in a feline model of reperfusion-ischemia prevented neutrophil accumulation and endothelial dysfunction, and reduced myocardial necrosis(Ma et al., 1993)	Yet to be established.
<i>Signal transduction & cell-interactions</i>			
TIE2	Receptor that is activated after binding of angiopoietin-1 and exerts mainly anti-inflammatory properties by promoting vascular integrity(Smith, Van Slyke, Jones, Dumont, & McGlade, 2018)		Elevated levels were associated with HFpEF(Berezin, Kremzer, Martovitskaya, Berezina, & Gromenko, 2016) and higher in MI and HFrEF vs. controls (Chong, Caine, Freestone, Blann, & Lip, 2004; Lee, Lip, & Blann, 2004). The prognostic implications of TIE2 in MI and HF have yet to be studied.
SRC	Proto-oncogene that promotes survival, angiogenesis, proliferation and invasion (Dehm & Bonham, 2004)	Mediates BNP gene expression by endothelin-1 in human myocytes(He & LaPointe, 2001)	Upregulated in human failing hearts(Vitello, Du, Buttrick, & Walker, 2012)
SELE	A selectin cell adhesion molecule expressed on endothelial cells. Recruits leukocytes to the site of injury during inflammation or after shear stress (e.g. during ischemia/reperfusion injury(R. B. Huang & Eniola-Adefeso, 2012)).	Upregulated in the myocardium of HFPEF patients(Franssen et al., 2016)	Predicted mortality in diabetic HF patients(Czucz et al., 2011)

PDGFC	Activates several pathways promoting cell survival and angiogenesis(Medamana, Clark, & Butler, 2017)	Critical regulator of post-MI repair processes (including collagen deposition in the infarct)(Zymek et al., 2006) and PDGFC infusion enhanced post-ischemic revascularization of the heart in a murine model(Li et al., 2005).	Yet to be established.
ADGRG1	Plays a role in the early interaction between neurons and the pial basement membrane and hence in cerebral cortical development(Hamann et al., 2015) but also in other developmental processes such as muscle cell differentiation, male fertility, immune regulation and tumorigenesis(K. Y. Huang & Lin, 2018).	One of its ligands is collagen type III which plays a role in myocardial fibrosis (Luo et al., 2011)	Yet to be established.
FGF21	Family of signaling proteins that regulate reproduction, development and metabolism (glucose and lipid) by activating the FGF receptor family of membrane spanning receptor tyrosine kinases (Ornitz & Itoh, 2015).	Anti-inflammatory, anti-diabetic and hypolipidemic effects in animal studies(Woo, Xu, Wang, & Lam, 2013)	Elevated in metabolic disorders and CAD(Woo et al., 2013). High levels predict CV outcome in stable CAD (Ong et al., 2019) Hypothesis for differential effects in animal and clinical studies: potential FGF21 resistance in human disease(Ong et al., 2019).
<i>Metabolism</i>			
PCSK9	Binds the LDL receptor at the surface of hepatocytes which prevents LDL receptor recycling and hence reduces LDL-cholesterol clearance (Shimada & Cannon, 2015)		Elevated levels were associated with poor outcomes in MI and HFREF(Almontashiri et al., 2014; Bayes-Genis et al., 2017). Inhibition improved outcomes of patients with atherosclerosis and elevated LDL(Sabatine et al., 2017)

GH	Stimulates growth, reproduction and regeneration but also plays a role in maintaining the structure and function of the heart and regulating the vascular tone(Salzano et al., 2018)		GH deficiency is common in HFREF and associated with larger left ventricular volumes, higher filling pressures and higher mortality risk vs. HF patients with normal GH levels(Arcopinto et al., 2017). A GH deficiency is also observed in HFpEF patients, but to a lesser extent(Salzano et al., 2016). Our findings suggest an association in the other direction.
ENTPD2	Transmembrane protein expressed in the vasculature, mainly by microvascular pericytes, adventitial cells in muscularised vessels, and by distinct cell populations in the subendocardial space(Sevigny et al., 2002)	Promotes platelet microthrombus formation following vascular injury(Sevigny et al., 2002) and the attenuation of profibrotic nucleotide signaling in cardiac fibroblasts (Lu & Insel, 2013)	The role of ENTPD2 in human HF has yet to be established.

TNF, tumor necrosis factor; MI, myocardial infarction; HFREF, heart failure with reduced ejection fraction; HFPEF, heart failure with preserved ejection fraction; CAD, coronary artery disease; CMP, cardiomyopathy; SNPs single nucleotide polymorphisms, MI myocardial infarction, NSTEMI non-ST segment elevation myocardial infarction; BNP, brain natriuretic peptide; LDL, low-density lipoprotein; TIE2, angiopoietin-1 receptor; ENTPD2, ectonucleoside triphosphate diphosphohydrolase 2; CCL11, eotaxin; TNFSF13B, tumor necrosis factor ligand superfamily member 13B; PDGFC, platelet-derived growth factor C; SELL, L-selectin; PCSK9, proprotein convertase subtilisin/kexin type 9; TWEAK, tumor necrosis factor (Ligand) superfamily, member 12; NOS3, nitric oxide synthase; GNLY, granulysin; SELE, E-selectine; SERPINA9, serpin A9; AZU1, azurocidin; SRC, Proto-oncogene tyrosine-protein kinase Src; ADGRG1, adhesion G-protein coupled receptor G1; FGF-21, fibroblast growth factor 21; GH, growth hormone.

Figure 1

Network analyses for the visualization of pathways and protein-interactions between uncorrelated biomarkers with higher expressing in cluster 2 vs. cluster 1

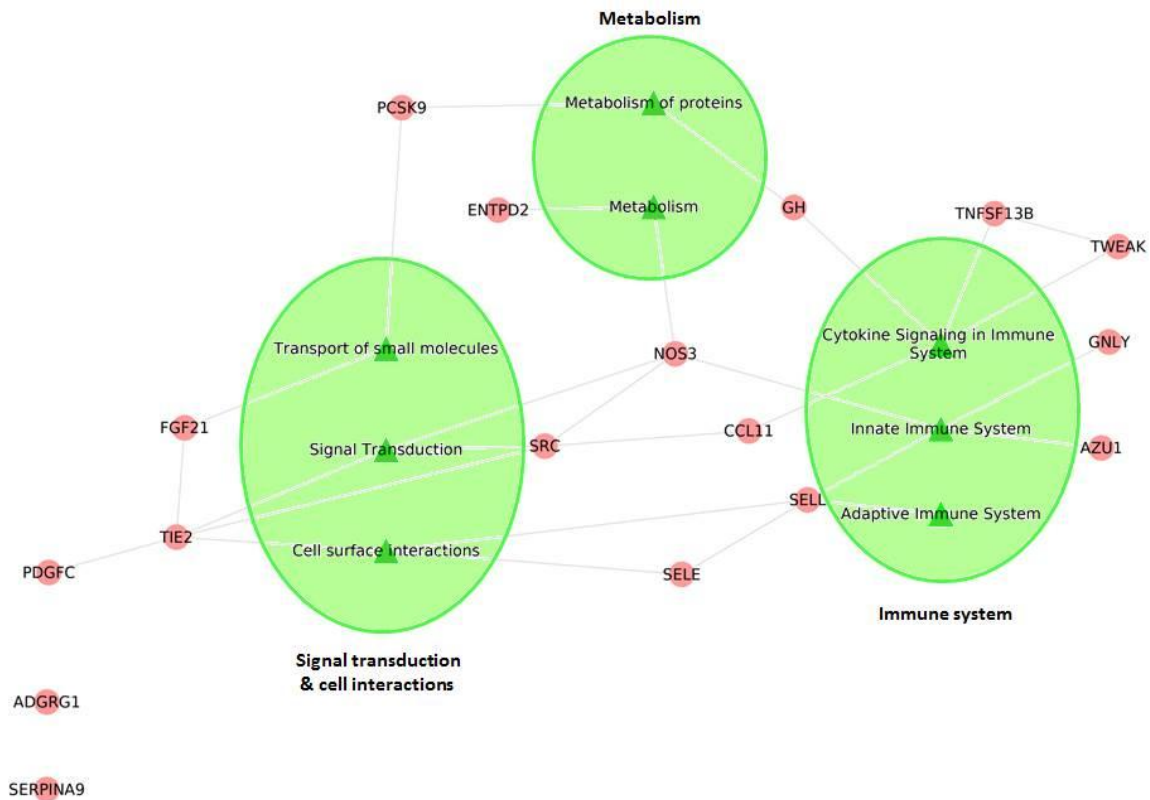
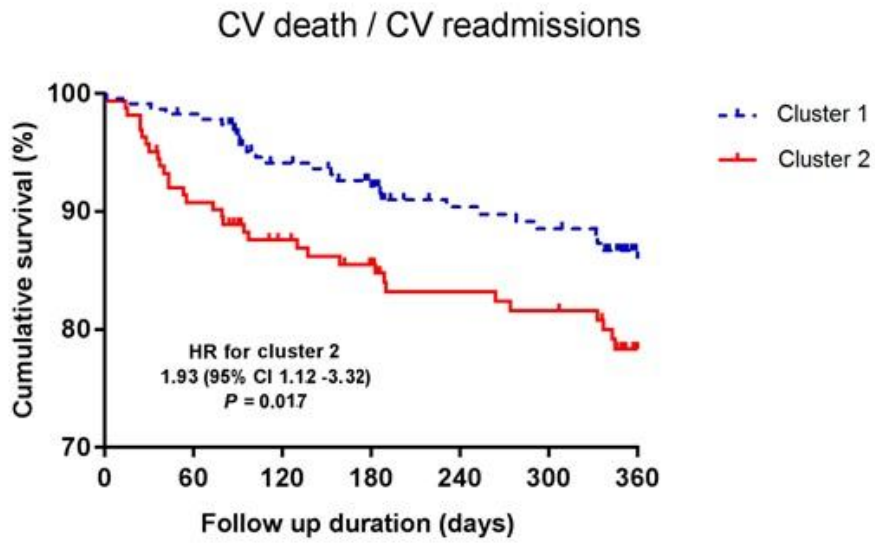


Figure legend. The FHF-GKB (Fight Heart Failure - Graph Knowledge Box) complex network was used to extract available knowledge about human protein-protein and protein-pathway relationships from public resources in order to explore pathways that could connect together biomarker nodes of interest. Queries were expressed according to query patterns defining a path structure between two nodes such as BM-BM and BM-pathway-BM and BM-pathway, where the BM nodes are taken from a list of interest. The resulting graphs were merged in a figure illustrating all possible paths not longer than two edges, connecting biomarkers through pathways and proteins. This graph depicts interactions between biomarkers: biomarker – biomarker, biomarker – pathway - biomarker and biomarker - pathway. Pink: biomarkers; Green: pathways. Two out of 17 biomarkers were not linked.

Figure 2

Event-free survival of patients according to cluster membership



No. at Risk

Cluster 1	229	225	194	184	149	146	126
Cluster 2	163	148	128	123	106	104	86

At baseline, echocardiography was performed in all patients and images were stored in a digital cine-loop format for off-line analysis following recommendations of the American Society of Echocardiography and the European Association of Cardiovascular Imaging relative to the cardiac chamber and right heart measurements¹

From standard 2D views, left ventricular (LV) structure and function were evaluated (including apical four-chamber, apical two-chamber and parasternal long- and short-axis views). Ventricular dimensions, wall thickness, mass and geometry were determined from 2D parasternal short- and long-axis views. LV volumes, stroke volume and ejection fraction were calculated using the biplane method (modified Simpson's rule). All cardiac chamber volumes and mass measurements were indexed to body surface area.

Left atrial (LA) volume was assessed by the biplane area-length method from apical 2- and 4-chamber views at end-systole and was indexed to body surface area (LA volume index, LAVi). LA area (cm²) was estimated from the apical views. If LA volume was not available, LA area was used to evaluate remodeling. Patients with either LAVi>40ml/m² or LA area>20cm² were considered to have dilated LA.

Pulsed-wave Doppler obtained at the tip of mitral leaflets was used to assess the peak velocities of early (E) and late (A) wave of transmitral flow and E-wave deceleration time (DT). The average of septal and lateral annular velocities (e') was measured using tissue Doppler imaging (TDI). The peak E-wave velocity and the average of septal and lateral e' were used to calculate the E/e' ratio. LV outflow tract (LVOT) time velocity integral, isovolumic relaxation time (IVRT) and color M-mode of early diastolic mitral inflow into the left ventricle (Flow propagation velocity, Vp) were acquired from apical four- and five-

¹ Lang RM *et al.* Recommendations for cardiac chamber quantification by echocardiography in adults: an update from the American Society of Echocardiography and the European Association of Cardiovascular Imaging. *Eur Heart J Cardiovasc Imaging* 2015; 16(3):233-70.

chamber views. Pulmonary venous flow (PVF) was sampled using pulsed-wave Doppler at 1 cm into the orifice of the right upper pulmonary vein.

TAPSE (in mm) measurement was performed to estimate right ventricular (RV) function and pulmonary arterial systolic pressure (PASP) was calculated using the peak velocity of tricuspid regurgitation (TR) and the maximum IVC diameter (IVC baseline) and respiratory variation (Ratio IVC inspiration / IVC baseline) measured 3 cm before merger with the right atrium.

Overall, echocardiographic data were complete in >75% of patients, except for A (and E/A ratio) (which were available in 70% and 61% of the population, respectively).

Supplemental table 1 ***Participating centers MEDIA-DHF***

Nancy Clinical Investigation Centre, University of Lorraine, France (and EDDH European Drug Development Hub, Nancy, France as project manager)
Lariboisière Hospital, Paris, France
Free University Medical Centre, Amsterdam, The Netherlands
CHARITE, universitätsmedizin Berlin, Berlin Germany
University of Porto, Porto, Portugal
University of Maastricht, Maastricht, The Netherlands
Hartcentrum ZNA, Antwerp, Belgium
Cardiff University, Cardiff, United Kingdom
Foundation for Applied Medical Research, Pamplona, Spain
University of Eastern PIEMONTE Medical School, Novara, Italy
University of Brescia, Brescia, Italy
University of Perugia, Perugia, Italy
University College Dublin, National University of Ireland, Dublin, Ireland
University Debrecen, Debrecen, Hungary
Oslo University Hospital, Norway

Supplemental table 2**Overview of biomarkers measured at baseline in MEDIA-DHF**

Organ damage panel	
5'-AMP-activated protein kinase subunit beta-1 (PRKAB1) Q9Y478	Kidney Injury Molecule (KIM1) Q96D42
Adhesion G-protein coupled receptor G1 (ADGRG1) Q9Y653	Leukotriene A-4 hydrolase (LTA4H) P09960
Aldehyde dehydrogenase, dimeric NADP-preferring (ALDH3A1) P30838	Linker for activation of T-cells family member 2 (LAT2) Q9GZY6
Anterior gradient protein 2 homolog (AGR2) O95994	Lutropin subunit beta (LHB) P01229
Apoptosis-inducing factor 1, mitochondrial (AIFM1) O95831	Macrophage erythroblast attacher (MAEA) Q7L5Y9
B-cell scaffold protein with ankyrin repeats (BANK1) Q8NDB2	Macrophage-capping protein (CAPG) P40121
BH3-interacting domain death agonist (BID) P55957	Melanoma-associated antigen D1 (MAGED1) Q9Y5V3
BMP and activin membrane-bound inhibitor homolog (BAMBI) Q13145	Methionine aminopeptidase 1 (METAP1) P53582
Calcitonin (CALCA) P01258	Mevalonate kinase (MVK) Q03426
Calreticulin (CALR) P27797	Mitogen-activated protein kinase kinase kinase kinase 5 (MAP4K5) Q9Y4K4
Carbonic anhydrase 12 (CA12) O43570	Mothers against decapentaplegic homolog 1 (SMAD1) Q15797
Carbonic anhydrase 14 (CA14) Q9ULX7	NAD-dependent protein deacylase sirtuin-5, mitochondrial (SIRT5) Q9NXA8
Casein kinase I isoform delta (CSNK1D) P48730	NEDD8 ultimate buster 1 (NUB1) Q9Y5A7
Claspin (CLSPN) Q9HAW4	Neutrophil cytosol factor 2 (NCF2) P19878
CMP-N-acetylneuraminase-beta-galactosamide-alpha-2,3-sialyltransferase 1 (ST3GAL1) Q11201	Nibrin (NBN) O60934
Cocaine esterase (CES2) O00748	Nitric oxide synthase, endothelial (NOS3) P29474
Contactin-2 (CNTN2) Q02246	Nucleobindin-2 (NUCB2) P80303
Corticoliberin (CRH) P06850	Parvalbumin alpha (PVALB) P20472
C-type lectin domain family 1 member A (CLEC1A) Q8NC01	Paxillin (PXN) P49023
C-type natriuretic peptide (NPPC) P23582	Peptidyl-prolyl cis-trans isomerase FKBP1B (FKBP1B) P68106
Desmoglein-4 (DSG4) Q86SJ6	Perilipin-1 (PLIN1) O60240
Dipeptidyl aminopeptidase-like protein 6 (DPP6) P42658	Placenta growth factor (PGF) P49763
DNA topoisomerase 2-beta (TOP2B) Q02880	Platelet-derived growth factor C (PDGFC) Q9NRA1
Ectonucleoside triphosphate diphosphohydrolase 2 (ENTPD2) Q9Y5L3	Pleiotrophin (PTN) P21246
Ectonucleoside triphosphate diphosphohydrolase 6 (ENTPD6) O75354	Phosphatidylinositol 3,4,5-trisphosphate 5-phosphatase 2 (INPPL1) O15357
EGF-like repeat and discoidin I-like domain-containing protein 3 (EDIL3) O43854	Plexin domain-containing protein 1 (PLXDC1) Q8IUU5
Enteropeptidase (TMPRSS15) P98073	Polypeptide N-acetylgalactosaminyltransferase 10 (GALNT10) Q86SR1
Epidermal growth factor-like protein 7 (EGFL7) Q9UHF1	Probetacellulin (BTC) P35070
Erbin (ERBIN) Q96RT1	Programmed cell death protein 1 (PDCD1) Q15116
Erythropoietin (EPO) P01588	Prolow-density lipoprotein receptor-related protein 1 (LRP1) Q07954
Fatty acid-binding protein 9 (FABP9) Q0Z7S8	Proteasome subunit alpha type-1 (PSMA1) P25786
Forkhead box protein O1 (FOXO1) Q12778	Protein amnionless (AMN) Q9BXJ7
Fructose-2,6-bisphosphatase TIGAR (TIGAR) Q9NQ88	Protein fosB (FOSB) P53539
Hematopoietic prostaglandin D synthase (HPGDS) O60760	Protein max (MAX) P61244
Inactive tyrosine-protein kinase 7 (PTK7) Q13308	Protein phosphatase 1B (PPM1B) O75688
Integrin beta-1-binding protein 1 (ITGB1BP1) O14713	[Pyruvate dehydrogenase [acetyl-transferring]]-phosphatase 1, mitochondrial (PDP1) Q9P0J1
Interferon-inducible double-stranded RNA-dependent protein kinase activator A (PRKRA) O75569	Ras association domain-containing protein 2 (RASSF2) P50749
Renin receptor (ATP6AP2) O75787	Ras GTPase-activating protein 1 (RASGAP1) P20936
	Receptor-type tyrosine-protein phosphatase eta (PTPRJ) Q12913
	EGF-containing fibulin-like extracellular matrix protein 1 (EFEMP1)

	Q12805
REST corepressor 1 (RCOR1) Q9UKL0	Endoglin (ENG) P17813
Retinoic acid receptor responder protein 1 (RARRES1) P49788	Fetuin-B (FETUB) Q9UGM5
Ribonucleoside-diphosphate reductase subunit M2 B (RRM2B) Q7LG56	Ficolin-2 (FCN2) Q15485
Serpin A9 (SERPINA9) Q86WD7	Glutaminyl-peptide cyclotransferase (QPCT) Q16769
Serum paraoxonase/arylesterase 2 (PON2) Q15165	Granulysin (GNLY) P22749
Syntaxin-8 (STX8) Q9UNK0	Growth arrest-specific protein 6 (GAS6) Q14393
Syntaxin-binding protein 3 (STXBP3) O00186	Hepatocyte growth factor receptor (MET) P08581
Troponin I, cardiac muscle (TNNI3) P19429	Ig lambda-2 chain C regions (IGLC2) P0CG05
Tyrosine-protein kinase Fes/Fps (FES) P07332	Insulin-like growth factor-binding protein 3 (IGFBP3) P17936
Tyrosine-protein kinase Fgr (FGR) P09769	Insulin-like growth factor-binding protein 6 (IGFBP6) P24592
Tyrosine-protein kinase Yes (YES1) P07947	Integrin alpha-M (ITGAM) P11215
Vascular endothelial growth factor C (VEGFC) P49767	Intercellular adhesion molecule 1 (ICAM1) P05362
Vasohibin-1 (VASH1) Q7L8A9	Intercellular adhesion molecule 3 (ICAM3) P32942
Wiskott-Aldrich syndrome protein (WAS) P42768	Interleukin-7 receptor subunit alpha (IL7R) P16871
	Latent-transforming growth factor beta-binding protein 2 (LTBP2) Q14767
Cardiometabolic panel	Leukocyte immunoglobulin-like receptor subfamily B member 1 (LILRB1) Q8NHL6
Angiogenin (ANG) P03950	Leukocyte immunoglobulin-like receptor subfamily B member 2 (LILRB2) Q8N423
Angiopoietin-related protein 3 (ANGPTL3) Q9Y5C1	Leukocyte immunoglobulin-like receptor subfamily B member 5 (LILRB5) O75023
Apolipoprotein M (APOM) O95445	Lithostathine-1-alpha (REG1A) P05451
Beta-Ala-His dipeptidase (CNDP1) Q96KN2	Liver carboxylesterase 1 (CES1) P23141
Beta-galactoside alpha-2,6-sialyltransferase 1 (ST6GAL1) P15907	Low affinity immunoglobulin gamma Fc region receptor II-a (FCGR2A) P12318
Cadherin-1 (CDH1) P12830	Low affinity immunoglobulin gamma Fc region receptor III-B (FCGR3B) O75015
Carbonic anhydrase 1 (CA1) P00915	L-selectin (SELL) P14151
Carbonic anhydrase 3 (CA3) P07451	Lymphatic vessel endothelial hyaluronic acid receptor 1 (LYVE1) Q9Y5Y7
Carbonic anhydrase 4 (CA4) P22748	Lysosomal Pro-X carboxypeptidase (PRCP) P42785
Cartilage acidic protein 1 (CRTAC1) Q9NQ79	Mannose-binding protein C (MBL2) P11226
Cartilage oligomeric matrix protein (COMP) P49747	Mast/stem cell growth factor receptor Kit (KIT) P10721
C-C motif chemokine 5 (CCL5) P13501	Membrane cofactor protein (CD46) P15529
C-C motif chemokine 14 (CCL14) Q16627	Membrane primary amine oxidase (AOC3) Q16853
C-C motif chemokine 18 (CCL18) P55774	Metalloproteinase inhibitor 1 (TIMP1) P01033
CD59 glycoprotein (CD59) P13987	Microfibrillar-associated protein 5 (MFAP5) Q13361
Coagulation factor VII (F7) P08709	Multiple epidermal growth factor-like domains protein 9 (MEGF9) Q9HIU4
Coagulation factor XI (F11) P03951	Neural cell adhesion molecule 1 (NCAM1) P13591
Collagen alpha-1(XVIII) chain (COL18A1) P39060	Neural cell adhesion molecule L1-like protein (CHL1) O00533
Complement C1q tumor necrosis factor-related protein 1 (C1QTNF1) Q9BXJ1	Neurogenic locus notch homolog protein 1 (NOTCH1) P46531
Complement C2 (C2) P06681	Neuropilin-1 (NRP1) O14786
Complement factor H-related protein 5 (CFHR5) Q9BXR6	Neutrophil defensin 1 (DEFA1) P59665
Complement receptor type 2 (CR2) P20023	Neutrophil gelatinase-associated lipocalin (LCN2) P80188
Cystatin-C (CST3) P01034	Nidogen-1 (NID1) P14543
Dipeptidyl peptidase 4 (DPP4) P27487	Oncostatin-M-specific receptor subunit beta (OSMR) Q99650

Peptidyl-glycine alpha-amidating monooxygenase (PAM) P19021	C-C motif chemokine 17 (CCL17) Q92583
Phospholipid transfer protein (PLTP) P55058	CD40 ligand (CD40-L) P29965
Plasma serine protease inhibitor (SERPINA5) P05154	Chymotrypsin C (CTRC) Q99895
Platelet glycoprotein Ib alpha chain (GP1BA) P07359	C-X-C motif chemokine 1 (CXCL1) P09341
Platelet-activating factor acetylhydrolase (PLA2G7) Q13093	Decorin (DCN) P07585
Plexin-B2 (PLXNB2) O15031	Dickkopf-related protein 1 (Dkk-1) O94907
Procollagen C-endopeptidase enhancer 1 (PCOLCE) Q15113	Fatty acid-binding protein, intestinal (FABP2) P12104
Prolyl endopeptidase FAP (FAP) Q12884	Fibroblast growth factor 21 (FGF-21) Q9NSA1
Receptor-type tyrosine-protein phosphatase S (PTPRS) Q13332	Fibroblast growth factor 23 (FGF-23) Q9GZV9
Regenerating islet-derived protein 3-alpha (REG3A) Q06141	Follistatin (FS) P19883
Serum amyloid A-4 protein (SAA4) P35542	Galectin-9 (Gal-9) O00182
SPARC-like protein 1 (SPARCL1) Q14515	Gastric intrinsic factor (GIF) P27352
Superoxide dismutase [Cu-Zn] (SOD1) P00441	Gastrotropin (GT) P51161
T-cell immunoglobulin and mucin domain-containing protein 4 (TIMD4) Q96H15	Growth hormone (GH) P01241
Tenascin (TNC) P24821	Growth/differentiation factor 2 (GDF-2) Q9UK05
Tenascin-X (TNXB) P22105	Heat shock 27 kDa protein (HSP 27) P04792
Thrombospondin-4 (THBS4) P35443	Heme oxygenase 1 (HO-1) P09601
Thyroxine-binding globulin (SERPINA7) P05543	Hydroxyacid oxidase 1 (HAOX1) Q9UJM8
Transcobalamin-2 (TCN2) P20062	Interleukin-1 receptor antagonist protein (IL-1ra) P18510
Transforming growth factor beta receptor type 3 (TGFB3) Q03167	Interleukin-1 receptor-like 2 (IL1RL2) Q9HB29
Transforming growth factor-beta-induced protein ig-h3 (TGFB1) Q15582	Interleukin-4 receptor subunit alpha (IL-4RA) P24394
Trypsin-2 (PRSS2) P07478	Interleukin-6 (IL6) P05231
Tyrosine-protein kinase receptor Tie-1 (TIE1) P35590	Interleukin-17D (IL-17D) Q8TAD2
Uromodulin (UMOD) P07911	Interleukin-18 (IL-18) Q14116
Vascular cell adhesion protein 1 (VCAM1) P19320	Interleukin-27 (IL-27) Q8NEV9,
Vasorin (VASN) Q6EMK4	Q14213
Vitamin K-dependent protein C (PROC) P04070	Kidney Injury Molecule (KIM1) Q96D42
	Lactoylglutathione lyase (GLO1) Q04760
Cardiovascular II panel	Lectin-like oxidized LDL receptor 1 (LOX-1) P78380
2,4-dienoyl-CoA reductase, mitochondrial (DECR1) Q16698	Leptin (LEP) P41159
A disintegrin and metalloproteinase with thrombospondin motifs 13 (ADAM-TS13) Q76LX8	Lipoprotein lipase (LPL) P06858
ADM (ADM) P35318	Low affinity immunoglobulin gamma Fc region receptor II-b (IgG Fc receptor II-b) P31994
Agouti-related protein (AGRP) O00253	Lymphotactin (XCL1) P47992
Alpha-L-iduronidase (IDUA) P35475	Macrophage receptor MARCO (MARCO) Q9UEW3
Angiopoietin-1 (ANG-1) Q15389	Matrix metalloproteinase-7 (MMP-7) P09237
Angiopoietin-1 receptor (TIE2) Q02763	Matrix metalloproteinase-12 (MMP-12) P39900
Angiotensin-converting enzyme 2 (ACE2) Q9BYF1	Melusin (ITGB1BP2) Q9UKP3
Bone morphogenetic protein 6 (BMP-6) P22004	Natriuretic peptides B (BNP) P16860
Brother of CDO (Protein BOC) Q9BWW1	NF-kappa-B essential modulator (NEMO) Q9Y6K9
Carbonic anhydrase 5A, mitochondrial (CA5A) P35218	Osteoclast-associated immunoglobulin-like receptor (hOSCAR) Q8IYS5
Carcinoembryonic antigen-related cell adhesion molecule 8 (CEACAM8) P31997	Pappalysin-1 (PAPPA) Q13219
Cathepsin L1 (CTSL1) P07711	Pentraxin-related protein PTX3 (PTX3) P26022
C-C motif chemokine 3 (CCL3) P10147	Placenta growth factor (PGF) P49763

Platelet-derived growth factor subunit B (PDGF subunit B) P01127	Caspase-3 (CASP-3) P42574
Poly [ADP-ribose] polymerase 1 (PARP-1) P09874	Cathepsin D (CTSD) P07339
Polymeric immunoglobulin receptor (PIgR) P01833	Cathepsin Z (CTSZ) Q9UBR2
Programmed cell death 1 ligand 2 (PD-L2) Q9BQ51	C-C motif chemokine 15 (CCL15) Q16663
Proheparin-binding EGF-like growth factor (HB-EGF) Q99075	C-C motif chemokine 16 (CCL16) O15467
Pro-interleukin-16 (IL16) Q14005	Note: New assay under development N/A
Prolargin (PRELP) P51888	C-C motif chemokine 24 (CCL24) O00175
Prostasin (PRSS8) Q16651	CD166 antigen (ALCAM) Q13740
Protein AMBP (AMBP) P02760	Chitinase-3-like protein 1 (CHI3L1) P36222
Proteinase-activated receptor 1 (PAR-1) P25116	Chitotriosidase-1 (CHIT1) Q13231
Protein-glutamine gamma-glutamyltransferase 2 (TGM2) P21980	Collagen alpha-1(I) chain (COL1A1) P02452
Proto-oncogene tyrosine-protein kinase Src (SRC) P12931	Complement component C1q receptor (CD93) Q9NPY3
P-selectin glycoprotein ligand 1 (PSGL-1) Q14242	Contactin-1 (CNTN1) Q12860
Receptor for advanced glycosylation end products (RAGE) Q15109	C-X-C motif chemokine 16 (CXCL16) Q9H2A7
Renin (REN) P00797	Cystatin-B (CSTB) P04080
Serine protease 27 (PRSS27) Q9BQR3	Elafin (PI3) P19957
Serine/threonine-protein kinase 4 (STK4) Q13043	Ephrin type-B receptor 4 (EPHB4) P54760
Serpin A12 (SERPINA12) Q8IW75	Epidermal growth factor receptor (EGFR) P00533
SLAM family member 5 (CD84) Q9UIB8	Epithelial cell adhesion molecule (Ep-CAM) P16422
SLAM family member 7 (SLAMF7) Q9NQ25	E-selectin (SELE) P16581
Sortilin (SORT1) Q99523	Fatty acid-binding protein, adipocyte (FABP4) P15090
Spondin-2 (SPON2) Q9BUD6	Galectin-3 (Gal-3) P17931
Stem cell factor (SCF) P21583	Galectin-4 (Gal-4) P56470
Superoxide dismutase [Mn], mitochondrial (SOD2) P04179	Granulins (GRN) P28799
T-cell surface glycoprotein CD4 (CD4) P01730	Growth/differentiation factor 15 (GDF-15) Q99988
Thrombomodulin TM P07204	Insulin-like growth factor-binding protein 1 (IGFBP-1) P08833
Thrombopoietin (THPO) P40225	Insulin-like growth factor-binding protein 2 (IGFBP-2) P18065
Thrombospondin-2 (THBS2) P35442	Insulin-like growth factor-binding protein 7 (IGFBP-7) Q16270
Tissue factor (TF) P13726	Integrin beta-2 (ITGB2) P05107
TNF-related apoptosis-inducing ligand receptor 2 (TRAIL-R2) O14763	Intercellular adhesion molecule 2 (ICAM-2) P13598
Tumor necrosis factor receptor superfamily member 10A (TNFRSF10A) O00220	Interleukin-1 receptor type 1 (IL-1RT1) P14778
Tumor necrosis factor receptor superfamily member 11A (TNFRSF11A) Q9Y6Q6	Interleukin-1 receptor type 2 (IL-1RT2) P27930
Tumor necrosis factor receptor superfamily member 13B (TNFRSF13B) O14836	Interleukin-2 receptor subunit alpha (IL2-RA) P01589
Tyrosine-protein kinase Mer (MERTK) Q12866	Interleukin-6 receptor subunit alpha (IL-6RA) P08887
Vascular endothelial growth factor D (VEGFD) O43915	Interleukin-17 receptor A (IL-17RA) Q96F46
V-set and immunoglobulin domain-containing protein 2 (VSIG2) Q96IQ7	Interleukin-18-binding protein (IL-18BP) O95998
Cardiovascular III panel	Junctional adhesion molecule A (JAM-A) Q9Y624
Aminopeptidase N (AP-N) P15144	Kallikrein-6 (KLK6) Q92876
Azurocidin (AZU1) P20160	Low-density lipoprotein receptor (LDL receptor) P01130
Bleomycin hydrolase (BLM hydrolase) Q13867	Lymphotoxin-beta receptor (LTBR) P36941
Cadherin-5 (CDH5) P33151	Matrix extracellular phosphoglycoprotein (MEPE) Q9NQ76
Carboxypeptidase A1 (CPA1) P15085	Matrix metalloproteinase-2 (MMP-2) P08253
Carboxypeptidase B (CPB1) P15086	Matrix metalloproteinase-3 (MMP-3) P08254

Matrix metalloproteinase-9 (MMP-9) P14780	von Willebrand factor (vWF) P04275
Metalloproteinase inhibitor 4 (TIMP4) Q99727	
Monocyte chemotactic protein 1 (MCP-1) P13500	Inflammation panel
Myeloblastin (PRTN3) P24158	Adenosine Deaminase (ADA) P00813
Myeloperoxidase (MPO) P05164	Artemin (ARTN) Q5T4W7
Myoglobin (MB) P02144	Axin-1 (AXIN1) O15169
Neurogenic locus notch homolog protein 3 (Notch 3) Q9UM47	Beta-nerve growth factor (Beta-NGF) P01138
N-terminal prohormone brain natriuretic peptide (NT-proBNP) NA	Caspase-8 (CASP-8) Q14790
Osteopontin (OPN) P10451	C-C motif chemokine 3 (CCL3) P10147
Osteoprotegerin (OPG) O00300	C-C motif chemokine 4 (CCL4) P13236
Paraoxonase (PON3) Q15166	C-C motif chemokine 19 (CCL19) Q99731
Peptidoglycan recognition protein 1 (PGLYRP1) O75594	C-C motif chemokine 20 (CCL20) P78556
Perlecan (PLC) P98160	C-C motif chemokine 23 (CCL23) P55773
Plasminogen activator inhibitor 1 (PAI) P05121	C-C motif chemokine 25 (CCL25) O15444
Platelet endothelial cell adhesion molecule (PECAM-1) P16284	C-C motif chemokine 28 (CCL28) Q9NRJ3
Platelet-derived growth factor subunit A (PDGF subunit A) P04085	CD40L receptor (CD40) P25942
Proprotein convertase subtilisin/kexin type 9 (PCSK9) Q8NBP7	CUB domain-containing protein 1 (CDCP1) Q9H5V8
Protein delta homolog 1 (DLK-1) P80370	C-X-C motif chemokine 1 (CXCL1) P09341
P-selectin (SELP) P16109	C-X-C motif chemokine 5 (CXCL5) P42830
Pulmonary surfactant-associated protein D (PSP-D) P35247	C-X-C motif chemokine 6 (CXCL6) P80162
Resistin (RETN) Q9HD89	C-X-C motif chemokine 9 (CXCL9) Q07325
Retinoic acid receptor responder protein 2 (RARRES2) Q99969	C-X-C motif chemokine 10 (CXCL10) P02778
Scavenger receptor cysteine-rich type 1 protein M130 (CD163) Q86VB7	C-X-C motif chemokine 11 (CXCL11) O14625
Secretoglobin family 3A member 2 (SCGB3A2) Q96PL1	Cystatin D (CST5) P28325
Spondin-1 (SPON1) Q9HCB6	Delta and Notch-like epidermal growth factor-related receptor (DNER) Q8NFT8
ST2 protein (ST2) Q01638	Eotaxin (CCL11) P51671
Tartrate-resistant acid phosphatase type 5 (TR-AP) P13686	Eukaryotic translation initiation factor 4E-binding protein 1 (4E-BP1) Q13541
Tissue factor pathway inhibitor (TFPI) P10646	Fibroblast growth factor 21 (FGF-21) Q9NSA1
Tissue-type plasminogen activator (t-PA) P00750	Fibroblast growth factor 23 (FGF-23) Q9GZV9
Transferrin receptor protein 1 (TR) P02786	Fibroblast growth factor 5 (FGF-5) Q8NF90
Trefoil factor 3 (TFF3) Q07654	Fibroblast growth factor 19 (FGF-19) O95750
Trem-like transcript 2 protein (TLT-2) Q5T2D2	Fms-related tyrosine kinase 3 ligand (Flt3L) P49771
Tumor necrosis factor ligand superfamily member 13B (TNFSF13B) Q9Y275	Fractalkine (CX3CL1) P78423
Tumor necrosis factor receptor 1 (TNF-R1) P19438	Glial cell line-derived neurotrophic factor (GDNF) P39905
Tumor necrosis factor receptor 2 (TNF-R2) P20333	Hepatocyte growth factor (HGF) P14210
Tumor necrosis factor receptor superfamily member 6 (FAS) P25445	Interferon gamma (IFN-gamma) P01579
Tumor necrosis factor receptor superfamily member 10C (TNFRSF10C) O14798	Interleukin-1 alpha (IL-1 alpha) P01583
Tumor necrosis factor receptor superfamily member 14 (TNFRSF14) Q92956	Interleukin-2 (IL-2) P60568
Tyrosine-protein kinase receptor UFO (AXL) P30530	Interleukin-2 receptor subunit beta (IL-2RB) P14784
Tyrosine-protein phosphatase non-receptor type substrate 1 (SHPS-1) P78324	Interleukin-4 (IL-4) P05112
Urokinase plasminogen activator surface receptor (U-PAR) Q03405	Interleukin-5 (IL5) P05113
Urokinase-type plasminogen activator (uPA) P00749	Interleukin-6 (IL6) P05231

Interleukin-7 (IL-7) P13232	Thymic stromal lymphopoietin (TSLP) Q969D9
Interleukin-8 (IL-8) P10145	TNF-related activation-induced cytokine (TRANCE) O14788
Interleukin-10 (IL10) P22301	TNF-related apoptosis-inducing ligand (TRAIL) P50591
Interleukin-10 receptor subunit alpha (IL-10RA) Q13651	Transforming growth factor alpha (TGF-alpha) P01135
Interleukin-10 receptor subunit beta (IL-10RB) Q08334	Tumor necrosis factor (Ligand) superfamily, member 12(TWEAK) O43508
Interleukin-12 subunit beta (IL-12B) P29460	Tumor necrosis factor (TNF) P01375
Interleukin-13 (IL-13) P35225	Tumor necrosis factor ligand superfamily member 14 (TNFSF14) O43557
Interleukin-15 receptor subunit alpha (IL-15RA) Q13261	Tumor necrosis factor receptor superfamily member 9(TNFRSF9) Q07011
Interleukin-17A (IL-17A) Q16552	Urokinase-type plasminogen activator (uPA) P00749
Interleukin-17C (IL-17C) Q9P0M4	Vascular endothelial growth factor A (VEGF-A) P15692
Interleukin-18 (IL-18) Q14116	
Interleukin-18 receptor 1 (IL-18R1) Q13478	
Interleukin-20 (IL-20) Q9NYY1	
Interleukin-20 receptor subunit alpha (IL-20RA) Q9UHF4	
Interleukin-22 receptor subunit alpha-1 (IL-22 RA1) Q8N6P7	
Interleukin-24 (IL-24) Q13007	
Interleukin-33 (IL-33) O95760	
Latency-associated peptide transforming growth factor beta-1 (LAP TGF-beta-1) P01137	
Leukemia inhibitory factor (LIF) P15018	
Leukemia inhibitory factor receptor (LIF-R) P42702	
Macrophage colony-stimulating factor 1 (CSF-1) P09603	
Matrix metalloproteinase-1 (MMP-1) P03956	
Matrix metalloproteinase-10 (MMP-10) P09238	
Monocyte chemotactic protein 1 (MCP-1) P13500	
Monocyte chemotactic protein 2 (MCP-2) P80075	
Monocyte chemotactic protein 3 (MCP-3) P80098	
Monocyte chemotactic protein 4 (MCP-4) Q99616	
Natural killer cell receptor 2B4 (CD244) Q9BZW8	
Neurotrophin-3 (NT-3) P20783	
Neurturin (NRTN) Q99748	
Oncostatin-M (OSM) P13725	
Osteoprotegerin (OPG) O00300	
Programmed cell death 1 ligand 1 (PD-L1) Q9NZQ7	
Protein S100-A12 (EN-RAGE) P80511	
Signaling lymphocytic activation molecule (SLAMF1) Q13291	
SIR2-like protein 2 (SIRT2) Q8IXJ6	
STAM-binding protein (STAMPB) O95630	
Stem cell factor (SCF) P21583	
Sulfotransferase 1A1 (ST1A1) P50225	
T cell surface glycoprotein CD6 isoform (CD6) Q8WWJ7	
T-cell surface glycoprotein CD5 (CD5) P06127	
T-cell surface glycoprotein CD8 alpha chain (CD8A) P01732	
TNF-beta (TNFB) P01374	

Supplemental table 3**Clinical variables in MEDIA-DHF**

Sex
Age
Recently decompensated (< 60 days) HF
Smoking status
Alcohol consumption
Body mass index (BMI)
Systolic blood pressure (SBP)
Diastolic blood pressure (DBP)
Pulmonary rales
New York Heart Association (NYHA)
Peripheral edema
Jugular Venous Distension
Fatigue on exertion
Hepatomegaly
Heart rate
Previous HF hospitalization
Atrial fibrillation
Hypertension
Diabetes Mellitus
Coronary Artery Disease (CAD)
Stroke or Transient Ischemic Attack
Peripheral arterial disease
Chronic obstructive pulmonary disease
Total cholesterol
Anemia (defined as hemoglobin <12 g/dL in women and <13 g/dL following WHO definition)
Estimated glomerular filtration rate (MDRD)
ACE inhibitor or angiotensin receptor blocker
Betablocker
Loop diuretic
Thiazide diuretic
Mineralocorticoid receptor antagonist
Oral anticoagulant
Insulin
Statin
Left ventricular ejection fraction (LV
LV end-diastolic index (LVEDVi)
LV end-systolic volume index (LVESVi),
left atrial volume index (LAVi),
tricuspid annular plane systolic excursion (TAPSE)
ratio of early mitral inflow E to annular velocity e' (E/e').
Excluded variables ($\geq 20\%$ missing)
pulmonary artery systolic pressure (PASP)
Ratio of the early (E) to late (A) ventricular filling velocities (E/A)
Waist circumference
Sodium
Potassium
CRP

Supplemental table 4 **Average measure of biomarkers according to respective clusters**

	Cluster 1 (N=229)	Cluster 2 (N=163)	p-value
TIE2	7.1 ± 0.3	7.3 ± 0.2	<0.001
ENTPD2	0.0 ± 0.2	0.1 ± 0.3	<0.001
CCL11	7.5 ± 0.4	7.8 ± 0.4	<0.001
TNFSF13B	5.7 ± 0.4	6.0 ± 0.5	<0.001
PDGFC	2.2 ± 0.4	2.3 ± 0.3	<0.001
SELL	7.5 ± 0.4	7.6 ± 0.4	0.006
PCSK9	1.8 ± 0.4	2.0 ± 0.4	<0.001
TWEAK	9.0 ± 0.5	9.1 ± 0.4	0.002
NOS3	1.3 ± 0.6	1.7 ± 0.6	<0.001
GNLY	0.5 ± 0.4	0.7 ± 0.5	<0.001
SELE	12.1 ± 0.6	12.3 ± 0.7	<0.001
SERPINA9	2.4 ± 0.6	2.8 ± 0.8	<0.001
AZU1	3.4 ± 0.8	3.8 ± 1.2	<0.001
SRC	6.5 ± 1.2	6.9 ± 1.0	0.001
ADGRG1	1.4 ± 1.0	2.2 ± 1.3	<0.001
FGF_21	5.7 ± 1.2	6.6 ± 1.5	<0.001
GH	7.6 ± 1.7	8.5 ± 1.6	<0.001

Legend: TIE2, angiotensin-1 receptor; ENTPD2, ectonucleoside triphosphate diphosphohydrolase 2; CCL11, eotaxin; TNFSF13B, tumor necrosis factor ligand superfamily member 13B; PDGFC, platelet-derived growth factor C; SELL, L-selectin; PCSK9, proprotein convertase subtilisin/kexin type 9; TWEAK, tumor necrosis factor (Ligand) superfamily, member 12; NOS3, nitric oxide synthase; GNLY, granulysin; SELE, E-selectine; SERPINA9, serpin A9; AZU1, azurocidin; SRC, Proto-oncogene tyrosine-protein kinase Src; ADGRG1, adhesion G-protein coupled receptor G1; FGF_21_1, fibroblast growth factor 21; GH, growth hormone.

Biomarker results depict log₂-normalized protein expression (NPX) data and an increase of 1 NPX confers therefore a doubling in concentration of the specific biomarker. For every biomarker the mean and standard deviation are listed.

Supplemental table 5**Crude and adjusted hazards ratios for the baseline prediction of cardiovascular death and/or cardiovascular hospitalization at 1 year in MEDIA-DHF**

	UNIVARIATE ANALYSES		MULTIVARIATE ANALYSES	
	HR (95% CI)	p-value	HR (95% CI)	p-value
Pulmonary rales	2.28 (1.34-3.86)	0.002	2.14 (1.25-3.68)	0.006
History of CAD	1.78 (1.06-2.99)	0.028	1.96 (1.15-3.42)	0.013
Previous HF hospitalization	1.75 (1.06-2.91)	0.030		
eGFR < 60 mL/min/1.73m ²	1.51 (1.30-1.76)	<0.001		
Anemia	1.50 (1.28-1.75)	<0.001		
E/e' > 9	3.37 (2.48-4.58)	<0.001		
Age (per 10 years)	1.00 (0.76-1.31)	0.99	0.93 (0.70-1.22)	0.59
Female sex	1.26 (0.73-2.16)	0.41	1.48 (0.83-2.63)	0.18

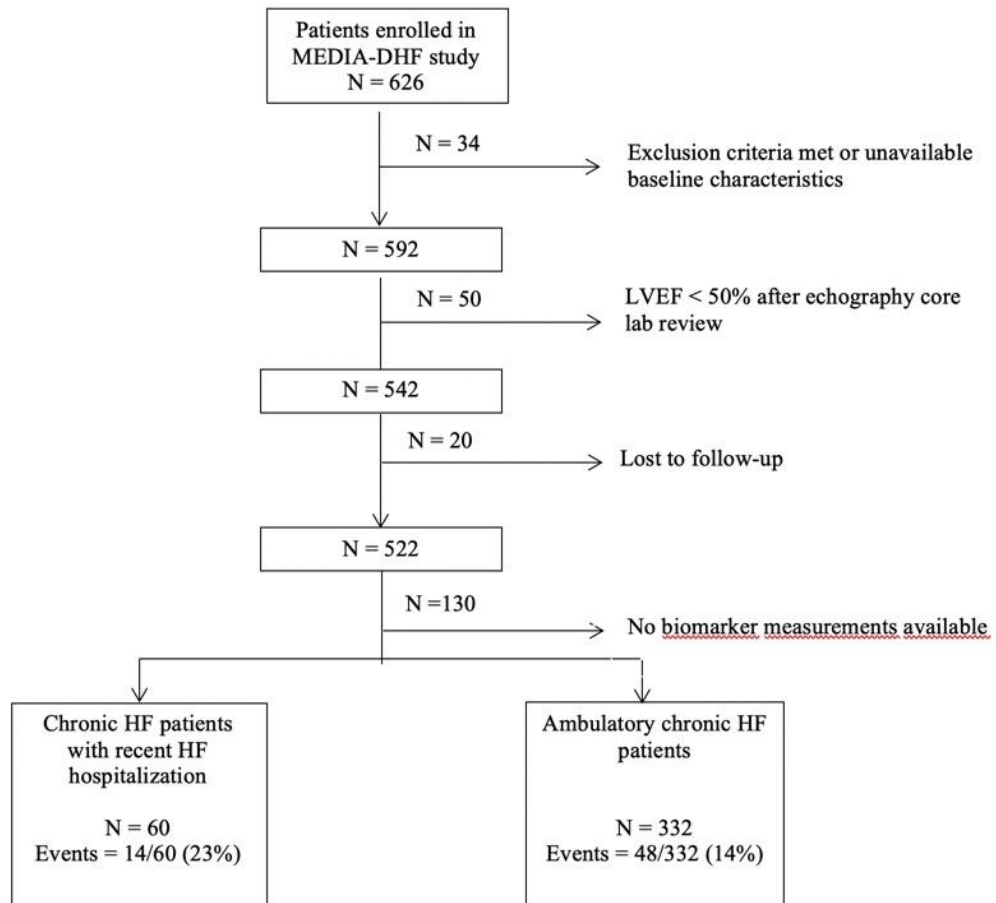
The table depicts pooled estimates derived after multiple imputation in 10 datasets. Anemia is defined following the WHO criteria for anemia (Hb < 12 g/dl in women; Hb < 13 in males).

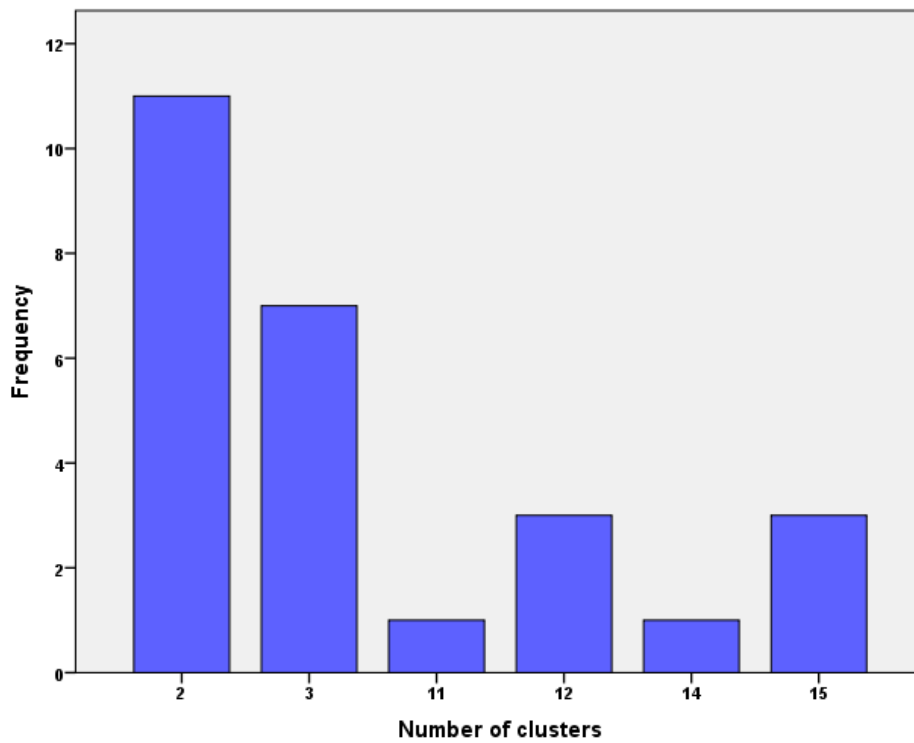
Legend: HR, hazard ratio; CI, confidence interval; CAD, coronary artery disease; HF, heart failure; eGFR, estimated glomerular filtration rate; E/E', the ratio of early mitral inflow E to e'

Supplemental table 6

Association between cluster assignment and cardiovascular outcomes after adjustment for additional clinical variables

	Additional adjusted variables on top of clinical + cluster model									
	Clinical	Clinical + cluster	+ prev HF hosp	+ anemia	+ SBP	NYHA 3/4	DM 2	ACE/ARB	BB	MRA
	HR (95% CI)	HR (95% CI)	HR (95% CI)	HR (95% CI)	HR (95% CI)	HR (95% CI)	HR (95% CI)	HR (95% CI)	HR (95% CI)	HR (95% CI)
Pulmonary rales	2.14 (1.25-3.68) p=0.006	2.17 (1.26-3.72) P=0.005	2.14 (1.24-3.67) P=0.006	2.85 (1.61-5.01) P<0.001	2.24 (1.29-3.88) P=0.004	2.19 (1.27-3.78) P=0.005	2.12 (1.23-3.66) P=0.007	2.19 (1.27-3.76) P=0.005	2.10 (1.22-3.63) P=0.008	2.17 (1.27-3.73) P=0.01
History of CAD	1.96 (1.15-3.42) p=0.013	2.01 (1.26-3.46) P=0.012	1.88 (1.09-3.26) P=0.024	1.84 (1.02-3.31) P=0.04	1.83 (1.05-3.20) P=0.034	2.05 (1.18-3.56) P=0.011	1.98 (1.15-3.42) P=0.014	2.02 (1.17-3.49) P=0.01	1.95 (1.12-3.38) P=0.02	2.02 (1.17-3.49) P=0.01
Age (per 10 years)	0.93 (0.70-1.22) p=0.059	0.86 (0.65-1.13) P=0.27	0.85 (0.65-1.12) P=0.26	0.86 (0.63-1.17) P=0.34	0.88 (0.66-1.17) P=0.38	0.84 (0.64-1.12) P=0.23	0.87 (0.66-1.16) P=0.36	0.85 (0.64-1.13) P=0.26	0.87 (0.65-1.15) P=0.33	0.87 (0.65-1.14) P=0.31
Female sex	1.48 (0.83-2.63) P=0.018	1.68 (0.93-3.02) P=0.085	1.80 (0.99-3.26) 0.053	1.51 (0.80-2.89) P=0.34	1.71 (0.93-3.12) P=0.083	1.65 (0.91-2.98) P=0.09	1.70 (0.94-3.08) P=0.08	1.69 (0.94-3.04) P=0.08	1.69 (0.94-3.04) P=0.08	1.67 (0.92-3.00) P=0.09
Cluster 2		1.93 (1.12-1.32) P=0.018	1.81 (1.05-3.13) P=0.033	1.69 (0.93-3.07) P=0.087	2.04 (1.17-3.57) P=0.012	1.84 (1.06-3.19) P=0.029	1.90 (1.10-3.27) P=0.021	1.90 (1.10-3.28) P=0.02	1.86 (1.08-3.23) P=0.03	1.99 (1.15-3.42) P=0.01
Previous HF hosp			1.53 (0.89-2.65) P=0.13)							
Anemia				1.21 (0.67-2.16) 0.53						
SBP					0.99 (0.98-1.01) P=0.83					
NYHA 3 / 4						1.23 (0.65-2.31) P=0.53				
DM type 2							1.21 (0.71-2.08) P=0.49			
ACE/ARB								0.84 (0.45-1.58) P=0.59		
BB									1.29 (0.65-2.56) P=0.47	
MRA										0.60 (0.24-1.52) P=0.28





The optimal number of clusters determined by the *NbClust* package in R was 2. This package uses a total of 30 indices for determining the most optimal number of clusters from the results obtained by varying combinations of number of clusters, distance measures and clustering methods

